

Article

Design of a 2DOF-PID Control Scheme for Frequency/Power Regulation in a Two-Area Power System Using Dragonfly Algorithm with Integral-Based Weighted Goal Objective

Alaa M. Abdel-hamed ¹, Almoataz Y. Abdelaziz ² and Adel El-Shahat ^{3,*}

¹ Electrical Power and Machines Department, High Institute of Engineering, El-Shorouk Academy, Cairo 11837, Egypt

² Faculty of Engineering and Technology, Future University in Egypt, Cairo 11835, Egypt

³ Energy Technology Program, School of Engineering Technology, Purdue University, West Lafayette, IN 47907, USA

* Correspondence: asayedah@purdue.edu

Abstract: The increase in power demand, nonlinearity, complexity, varying structure, and other important causes has necessitated the implementation of artificial intelligent control methodologies for safe and acceptable operation of the electric power systems. Therefore, in this article, an improved two-degrees-of-freedom (2DOF-PID) control scheme is proposed for power/frequency control of a two-area interconnected electric power system. The parameters of the 2-DOF-PID control scheme are optimized using the Dragonfly Algorithm (DA) via a new integral-based weighted goal fitness function (IB-WGFF) (i.e., DF-2DOF-PID-IB-WGFF). The superiority of the suggested scheme is proved by comparing the results obtained using the proposed IB-WGFF with those obtained using the conventional controllers, and the 2DOF-PID controllers optimized using the DA and Genetic Algorithm (GA) via the frequently published performance criterion. To verify the stability, efficacy, and robustness of the proposed control scheme, a load disturbances and parameters perturbations with various percentages are implemented in the controlled system under the same controllers. Finally, verification results proved that the proposed 2DOF-PID optimized using DA via the IB-WGFF is more stable, efficient, and robust than the other controllers recently used in the literature.

Keywords: optimal control; Dragonfly Algorithm (DA); integral-based weighted goal fitness function I-BWGFF; 2-DOF-PID



Citation: Abdel-hamed, A.M.; Abdelaziz, A.Y.; El-Shahat, A. Design of a 2DOF-PID Control Scheme for Frequency/Power Regulation in a Two-Area Power System Using Dragonfly Algorithm with Integral-Based Weighted Goal Objective. *Energies* **2023**, *16*, 486. <https://doi.org/10.3390/en16010486>

Academic Editor: Faqiang Wang

Received: 17 November 2022

Revised: 19 December 2022

Accepted: 28 December 2022

Published: 2 January 2023



Copyright: © 2023 by the authors. Licensee MDPI, Basel, Switzerland. This article is an open access article distributed under the terms and conditions of the Creative Commons Attribution (CC BY) license (<https://creativecommons.org/licenses/by/4.0/>).

1. Introduction

A modern Power System (PS) is a dynamic behavior system where interactive dynamic elements connected via power lines. Its function is to supply power to various loads or ensemble of consumers as a one from its critical various parts [1,2].

For a power system to operate in stability region, both the tie-line power deviation (ΔP) and system frequency (Δf) had to be constant. The Frequency variation effects badly the speed of electric devices in power system such as induction and synchronous motors. High magnetizing currents in induction motors and transformers may be appear from the drop in frequency. Controlling the frequency and tie-line power, to be at their normal rated values, is a complex and difficult task for the variable nature of the power demand. The frequency/power deviation causes various undesired harms such as instability problems. The power system stability and its dynamic performance can be enhanced successfully by controlling the frequency/power via accurate design of Automatic Generation Control (AGC) or Load Frequency Control (LFC) scheme. The AGC is needed to ensure synchronization and for maintaining the frequency and tie-line power of a power system within their nominal values during load variations [3,4].

Many control methodologies have been recommended for addressing the concerns of AGC such as optimal, adaptive, and Artificial Intelligent (AI) methods [5]. Standard PID

controllers are frequently used to dress the power/frequency control for their simplicity, reliability, and the suitable ratio between cost and implementation performance [6]. The nonlinearity, uncertainties, and realistic aspects such as load disturbances of an interconnected power system increase instability problems in the power system [7]. The classical PID-controllers are implemented at the explicit or normal operating conditions. The nonlinearity characteristics in the interconnected real power systems makes the Conventional PID control not convenient in the fluctuating conditions, hence the PID controllers performance must be improved [8]. The artificial optimization search techniques are utilized efficiently for load frequency Control [9], deregulated LFC of multi-area power system via mine blast algorithm [10], and PID/FOPID-based Frequency control of zero-carbon multi-sources based interconnected power systems under deregulated scenarios [11]. Various improved control strategies for LFC have been suggested in the literature.

P. Praveena et al. in [12] presented an approach for selecting the parameters of the PID controller in LFC of a single area power system. They used the Ziegler-Nichols (ZN) and Genetic Algorithm (GA) for tuning the parameters of the suggested controller. Comparative study is presented using MATLAB Simulink. The simulation results indicated that the PID tuned via GA offers lower settling time and a zero steady-state error. No verification for the suggested controller are checked under load disturbances or parameters variation in the power system.

N. El Yakine et al. in [13] used a Particle Swarm Optimization (PSO) method for optimal tuning of the PID controllers used to control the LFC and the Automatic Voltage Regulator (AVR) in a two-area power system. The proposed control scheme controls separately, the reactive and active powers. The objective of their strategy is to suppress the system fluctuations resulting from disturbances and restore system's voltage and frequency to their nominal values. The obtained results using the suggested control are compared to the results obtained using Z-N method, GA, and Bacterial Foraging (BF) optimization methods. The authors, in their paper, used a step load disturbance, but a verification using various disturbances and parameters perturbations are not verified.

Yogendra Arya in [14] introduced a new fuzzy-PID with filter and double integral controller (FPID-II) for AGC of a two-area power system. The scaling factors of the proposed controller is tuned implementing the imperialist competitive algorithm using ISE performance criterion. The authors compared the proposed method's results with the results obtained using various Artificial Intelligent (AI) methods-based controllers. The scalability and efficacy of the proposed approach is proved by extending the study using a non-reheat thermal power system with nonlinearity and other different power system plants. The authors in this paper carried out a sensitivity analysis, under system parameters perturbations, to prove the robustness of the proposed approach, but no verification is carried out under variable disturbances and multiple load variations.

Devbrat Gupta et al. in [15] carried out a comparative study in integrated power system using Fractional Order (FO) ID, PID, and FOPI to control the power system under sudden disturbances in generations and loads. A GA is used to tune the controller gains. Simulation results proved that the FOPID controller is better in terms of the robustness and the frequency deviation.

Ruchika Lamba et al. in [16] proposed an interval FO-PID controller methodology for controlling the load frequency in a two-area interconnected power system. The stability boundary locus methodology is used to design the proposed controller. System parameters perturbation of ($\pm 50\%$) is checked using Kharitonov theorem instead of using fixed values. The turbine time-constant, governor constant, and load disturbance is changed while performing the analysis of the proposed controller. Simulation results illustrated that the proposed controller gives better performance than the conventional methods.

Rajveer Singh et al. in [17] used a 2DOF-PID controllers to control and analyze the frequency of two-area power system. The Month Moth Flame Optimization method (MFO) have been used to tune the parameters of the proposed controllers for minimizing the frequency deviation and the deviation in the tie-line power. The results obtained using

the 2DOF-PID are compared with the results obtained using the recent meta-heuristic technique. Results proved the superiority of the suggested controllers over the other controllers in terms of the frequency deviation and tie-line power deviation. The sensitivity and efficiency of the proposed controllers against parameter variation and varying load disturbance still need to be verified.

Appala Naidu et al. in [18] introduced a new 2DOF-PID control scheme to control the frequency of an inter-connected power system integrated with wind power generation. The used controller is optimized using the Crow Optimization (CO) technique. In the proposed method, several reference inputs for a secondary control of frequency loop are used. Results showed that the supposed controller gives better control than other controllers.

EL Yakine, N. [19] introduced a new fuzzy-PID controller to solve the AGC problem in a two-area power system. The DA is implemented to tune the proposed controller parameters including the gains of the PID and the scaling factors of the fuzzy logic. The suggested methodology is extended to be applicable for AC/DC multisource power system linked with AC tie-line and a HVDC transmission link. The result of the proposed approach is compared with the results obtained using the AGC used in the literature. The authors extended their approach to be used in a non-linear power system of three areas of AGC. The comparative study proved the effectiveness of the suggested strategy in enhancing the frequency, however the proposed scheme still needs tuning for the part associated with the shaping factor of the Fuzzy logic.

Dipayan Guha in [20] discussed the LFC associated with an interconnected power system implementing a new Quasi-Opositional-Based (QO) JAYA. The used approach enhances the speed of convergence and select the best optimal solutions of the LFC problem by housing the knowledge of QO-based learning. The effectiveness of the suggested QOJAYA scheme is verified by implementing it to a plant of two area with multi-sources and multi areas. The PI controller is tuned and applied initially as secondary control. A 2DOF-PID controller is tuned and applied to enhance the dynamic stability of the power system under study. The proposed approaches used the single valued-time based objective as the fitness function to be minimized for searching the optimal setting for the proposed controllers. Simulation results demonstrated the superiority of the proposed QOJAYA controller over the base JAYA and Teaching Learning (TL) based tuning method. Sensitivity analysis is investigated to verify the suggested controller robustness.

Watanabe, M. et al. in [21] presented an improved method for regulating the frequency of a two-area power system. The proposed method implements the cascade configuration related to tilt integral-derivative and the FO-PID with a filter controller. Integrated squared Error (ISE), Integrated Absolute Error (IAE), Integrated Time Weighted Absolute Error (ITAE), and Integrated Time weighted Squared Error (ITSE) performance criteria are implemented in the optimization method as the objective function used to track the frequency deviation. The results are validated at changing loads and the robustness is checked against various uncertainties in the power system. The results proved stable operation under the proposed controller without no need for complex design methodologies.

Based on the above discussion, this paper proposes a 2DOF-PID control scheme for regulating the frequency and power fluctuations in a two-area power system. The Dragonfly Algorithm (DA) is used to optimally design the proposed scheme. A novel Integral-Based-weighted Goal Fitness Function (IB-WGFF) is implemented as the objective function to be minimized for controlling the frequency/power of the two-area power system. The proposed 2DOF-PID control scheme using the IB-WGFF is compared with the conventional- 2DOF-PID controller and the 2DOF-PID optimized using Dragonfly Algorithm (DA) and Genetic Algorithm (GA) via the other recently implemented fitness functions in the literature for interconnected power systems. The robustness for the designed 2DOF-PID is verified by investigating sensitivity analysis implementing loading and parameters uncertainties.

The paper contributes the following:

- i. Design and implementation a 2-DOF-PID control scheme for power/frequency control of two-area interconnected electric power system.
- ii. Design and implementation of a novel IB-WGFF to tune the 2DOF-PID controller parameters using the DA and GA.
- iii. Demonstrate the superiority of the proposed scheme by comparing the results with those obtained using the frequently published fitness-based controllers.
- iv. Verifying the stability, efficacy, and robustness of the proposed approach under load disturbances and parameter perturbations under the same proposed control scheme.

The remaining sections of this article are organized as follows: The model of the interconnected power system is presented in Section 2. Section 3 presents the mathematical modelling of the DA used for tuning the parameters of the proposed 2DOF-PID control scheme. Section 4 provides the design of the proposed fitness function and implementation of the DA and GA for tuning the parameters of the 2DOF-PID controllers. Section 5 introduces the simulation results and discussions. Verification of the proposed 2DOF-PID control scheme is introduced in Section 6. Finally, the conclusion is provided in Section 7.

2. Complete System Modeling

This section describes a complete system model of the interconnected power system presented in this paper. The two-area power system investigated here is commonly applied in the literature for designing and analyzing the LFC of the inter-connected electric power system. The system model of the two-area electric power system, used to discuss and analyze the limits and issues from the LFC, is shown in Figure 1a–c. The two areas are shown in Figure 1a,b shows a LFC implemented in a single area power system. In this system, each area encompasses a speed governor, steam turbine, and generator of 2000 MW rating, and a nominal step load of 2000 MW applied at the time instant 5 s [22,23].

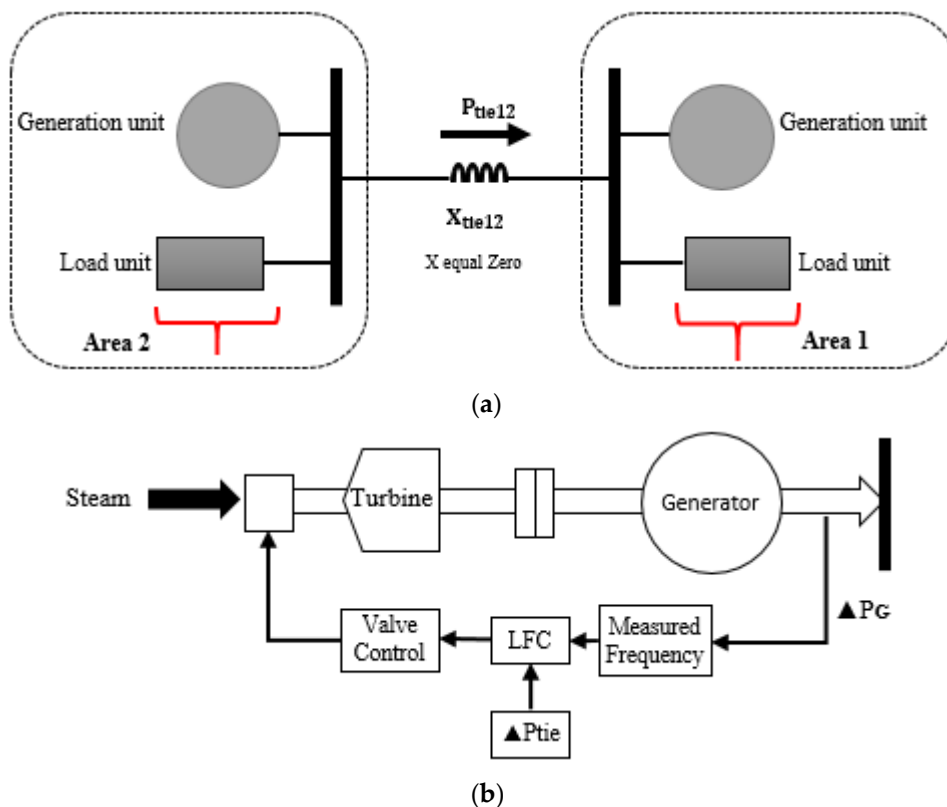


Figure 1. Cont.

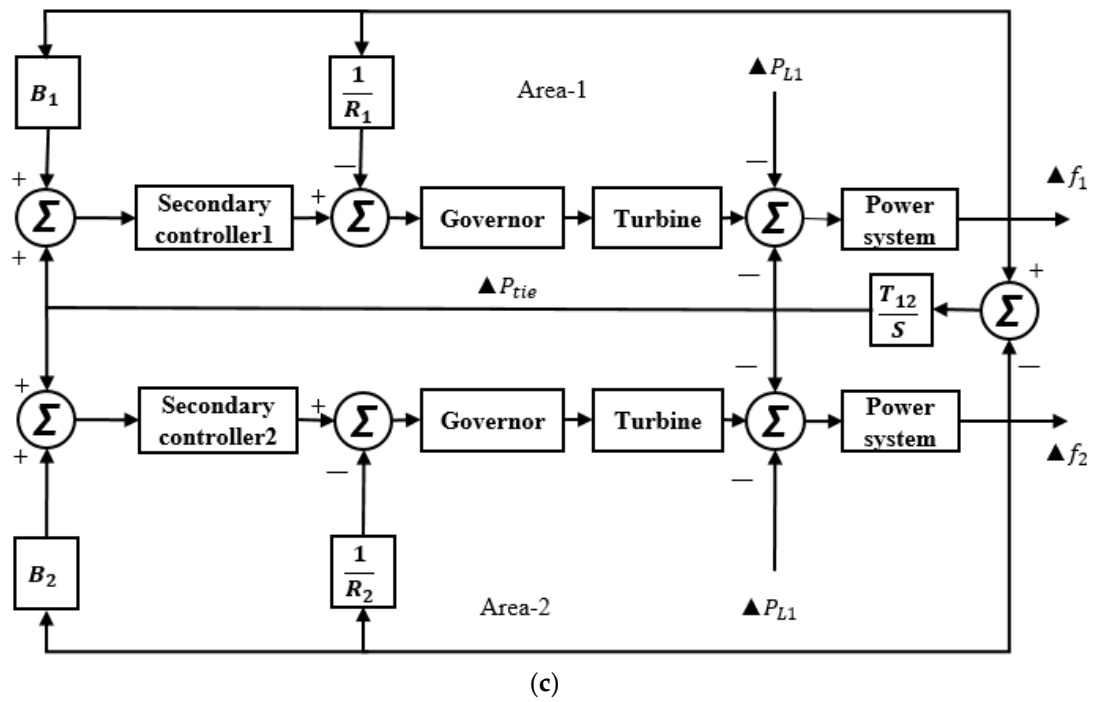


Figure 1. Circuit diagrams for the studied system (a) Circuit topology (b) LFC implemented a single area (c) Complete block diagram.

The non-linear equations used to describe the system-dynamic behavior can be linearized during load changes. In this case, a linearized model can be applied in the investigations [24]. The steam turbine can be modelled using the transfer function given by Equation (1).

$$G_t(s) = \frac{K_t}{T_t s + 1} \tag{1}$$

where T_t represents turbine time constant, K_t represents the turbine gain.

When the controlling system identifies frequency fluctuations, which may cause system instability, it will adjust the speed of the turbine for achieving the optimum speed that eliminates the frequency oscillations. The governor is modelled using the transfer function indicated by Equation (2) [25].

$$G_g(s) = \frac{K_g}{T_g s + 1} \tag{2}$$

where T_g represents governor time constant, K_g represents the governor gain.

The control action donated by the governor mechanism is given by Equation (3).

$$\Delta P_{ca} = \Delta P_r = \frac{1}{R} \Delta f \tag{3}$$

where ΔP_r is the set point change in power, Δf is the frequency change, R is the parameter of the speed governor regulator.

The load and the generator can be modelled using the transfer function described by Equation (4) [26,27].

$$G_{Sys}(s) = \frac{K_{ps}}{T_{ps} s + 1} \tag{4}$$

where $K_{ps} = \frac{1}{D}$ is the power system gain, $T_{ps} = \frac{2H}{fD}$ is the time constant of the power system, D represents the damping, and H represents the system inertia.

For each area of the selected power system, there are three inputs (i.e., the tie-line power deviation; ΔP_{tie} , load perturbation; ΔP_L , and controller input; ΔP_r) and two controlled outputs (i.e., the frequency deviation of the area 1; ΔP_{f1} , and the frequency deviation of area 2; ΔP_{f2}). The summation of the deviation in the tie-line power and frequency is defined by the control error (CE) of each area. The CEs are considered to be the input to the secondary controllers (i.e., the designed 2DOF-PID controllers) corresponding to their areas. CEs, used for the studied system shown in Figure 1, are indicated by Equations (5) and (6).

$$CE_1 = \Delta P_{tie} + B_1 \Delta f_1 \quad (5)$$

$$CE_2 = \Delta P_{tie} + B_2 \Delta f_2 \quad (6)$$

At steady state, CEs are the controlling signals used to reduce the frequency and power fluctuation to zero. Therefore, the 2DOF-PID controller must be designed for enhancing the transient of the dynamic system.

The complete system model with the controllers is shown in Figure 1c. The parameters used for the different components of the system is given in Table 1. As mentioned in Section 1, the variation of voltage level for the investigated power system is negligible with variation in load, as a result, filter impedance and the tie-line impedance between the system sources are neglected.

Table 1. Studied power system parameters.

Parameters	Values	Parameters	Values	Parameters	Values
R_1	2.4	D_2	0.90	B_1	20.1
D_1	-0.60	H_2	4.0	T_{12}	0.545
H_1	5.0	T_{g2}	0.30	R_2	0.0625
T_{g1}	0.20	T_{t2}	0.60	K_g	1.0
T_{t1}	0.50	B_2	16.90	K_t	1.0

2.1. DOF-PID Controller Modelling

The PID controller is still one of the most commonly used controllers in recent years due to its considered various advantages. These controllers work well even with uncertainty in the controlled systems. The mathematical model of the PID controllers is used as Equation (7) demonstrates: [14].

$$C(s) = \frac{Y(s)}{R(s)} = K_P + \frac{K_I}{S} + K_D S \quad (7)$$

The two-Degree of Freedom (2DOF-PID) controllers are commonly used to detect and control disturbance and rapid shock in electric power systems devoid of symbolic boost in set point tracking overshoot. Implementing the 2DOF-PID controllers can reduce the reference signal effect on the controlled electric power systems [28].

Figure 2 demonstrates the control architecture for the 2-DOF-PID controller in the controlled systems. The mathematical model used for the 2-DOF-PID controller is indicated by Equation (8).

$$U(s) = K_p(PW.R(s) - Y(s)) + \frac{K_i}{s}(R(s) - Y(s)) + \frac{K_d s}{N.s + 1}(DW.R(s) - Y(s)) \quad (8)$$

where $U(s)$ represents the controller output, $R(s)$ and $Y(s)$ represent the controller inputs, K_p is the proportional gain, K_i is the integral gain, K_d is the derivative gain, PW represents the reference weight of proportional gain, DW is the weight of the derivative, and N is the filter coefficient. In this paper, a FOPID control scheme is proposed for controlling the

frequency/power of a nonlinear interconnected power system, the FOPID control scheme is designed and validated.

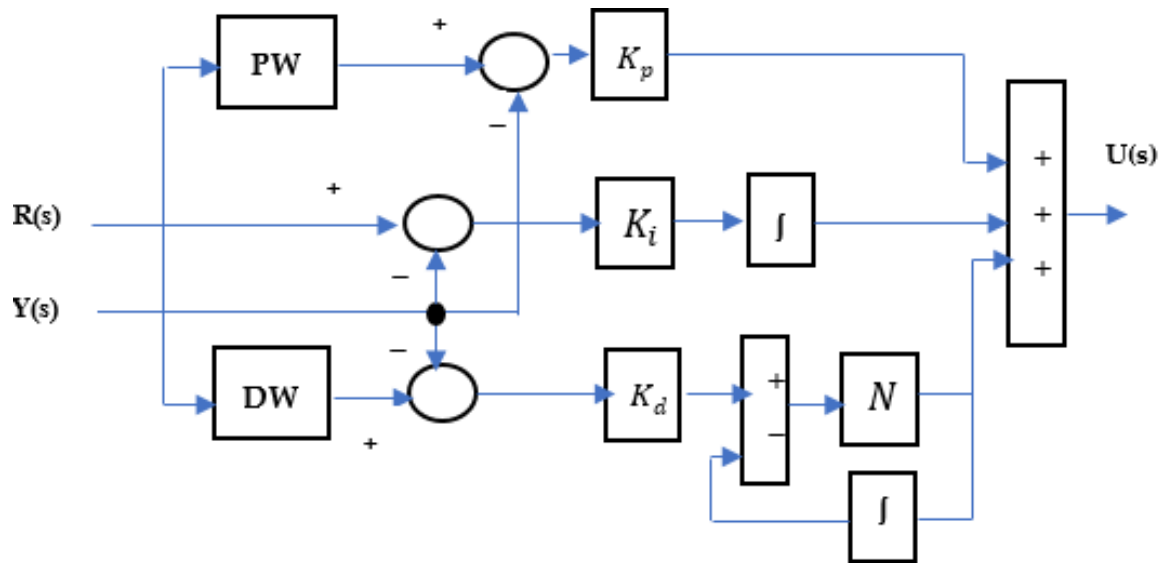


Figure 2. 2DOF-PID control architecture.

3. Dragonfly Algorithm (DA)

DA is proposed and designed by Mirjalili [29]. Dragonfly is mainly an optimization technique inspired by the dragonflies’ warming behavior which is static and dynamic. Its model is designed on the basis of the action, swarming dynamically or statically to find the foods and bypass enemies [30].

The static and dynamic swarm functions are considered to be two optimization stages which are called exploration and exploitation. In the exploration stage, phase dragonflies will build sub-swarms and will fly over several areas. This stage is the static swarms. In the exploitation phase, dragonflies will move in one strait direction for flying in larger swarms [31].

To model the flies’ motion, five characteristics of dragonflies are described here. These features are Separation (S_I), Alignment (A_I), Cohesion (C_I), Attraction of Food (AF_I), and Enemy (E_I). The five steps or features can be described and modelled mathematically as follows:

3.1. Separation (S_I)

For maximizing the population search space and avoiding collision, it is necessary for the distance between adjacent dragonflies to be within the specified or given locality. Assume I represents the number of individuals in a cluster and N represents the neighbors. The Separation (S_I) is modelled using Equation (9).

$$S_I = \sum_{K=1}^{K=N} (X - X_K) \tag{9}$$

where X is the dragonfly’s current positions, X_K is K^{th} neighboring’s position of dragonfly

3.2. Alignment (A_I)

The Alignment part (A_I) matches the individual’s velocity (V_K) with the other dragonflies with parallel velocity. Equation (10) models for the Alignment feature of the Dragonfly optimization algorithm.

$$A_I = \frac{\sum_{K=1}^{K=N} V_K}{N} \tag{10}$$

where V_K is the velocity for the K th neighboring dragonfly.

3.3. Cohesion (C_I)

All dragonfly's individuals in a cluster are motivated for moving in the path of center-mass of the neighboring dragonflies. The cohesion feature step (C_I) of dragonfly is modelled using Equation (11).

$$C_I = \frac{\sum_{K=1}^{K=N} V_K}{N} \quad (11)$$

3.4. Attraction of Food (AF_I)

In this feature, all individuals have a tendency for moving in food direction. The attraction for food (AF_I) feature at a location (X_F) is developed using Equation (12).

$$AF_I = X_F - X \quad (12)$$

3.5. Enemy (E_I)

In this step, all individuals in cluster have a tendency for moving away from the enemy. The mathematical model of the enemy feature (E_I) at the enemy location (X_E) can be designed using Equation (13).

$$E_I = X_E + X \quad (13)$$

The dragonflies' behavior in a cluster is affected by relating all the five features. The new updated position of the individual dragonflies indicated in Equation (14) is designed by step (ΔX_I) indicated by Equation (15).

$$X_I = X_I + \Delta X_I \quad (14)$$

$$\Delta X_I = (A.S_I + B.A_I + C.C_I + D.AF_I + E.E_I) + \omega \Delta X_I \quad (15)$$

where A , B , and C represent the weighted coefficients of the separation, alignment, and cohesion, respectively, while D represents the food coefficients and E is the enemy factor. ω Represents the inertial weighted coefficient. The exploitative and explorative variation performances of the dragonflies can be realized and modelled utilizing different values of coefficients.

4. Proposed Control Objective and Optimal Tuning of the 2DOF-PID Controller

4.1. Proposed Objective Function Formulation

The frequency and power fluctuations of interconnected power system are greatly affected by the consumer requests and the system parameter perturbations. These fluctuations make the frequency (Δf_a) and the tie line power (ΔP_{tie}) deviate from the nominal performance values accepted for stable power system.

A satisfactory level of stability in the controlled system and a fast behavior with speedily dampened fluctuations are desired in LFC. These requirements make the system have the capability of returning the frequency deviations (Δf_a) of each area and tie line power deviation (ΔP_{tie}) to the original or predetermined values.

A proper fitness/objective (FF) function should be designed and implemented before using recent optimization-based control schemes for achieving the best power/frequency performance [32]. There are many fitness/objective functions which have been implemented in the LFC problems found in the literature review, such as ITSE, ISE, IAE, and ITAE. All these fitness/objective functions have been used for restoring the normal operation or performance.

The ITAE and ISE performance criteria are applied in literature due to better performance in comparison with the ITSE and IAE performance criteria. The ISE criterion integrates the squared error over the simulation time. As the squared error has much bigger values, the ISE criterion may penalize great errors beyond smaller errors. The ITAE performance criterion integrates the absolute error over the simulation time. The ITAE

performance criterion will penalize errors and transients of long duration that occur later in the system responses [33–35].

Although The ITSE-optimized controllers minimized the contribution of initial errors and also assured errors later in the system response, they results of more time for settling in comparison with the ITAE-optimized controllers [6,33]. The ITAE-optimized controllers decreased the settling time better than the ISE, IAE, and ITSE-optimized controllers [6,33–35].

In the literature, the used fitness/objective function is the integral performance index type. Equations (16)–(19) demonstrates the ITSE, ISE, IAE and the ITAE fitness/objective functions used in the literature, respectively.

$$FF = ITSE = \int_0^t \left[\left(\sum_{a=1}^z \Delta f_a \right)^2 + (\Delta P_{tie})^2 \right] .t.dt \quad (16)$$

$$FF = ISE = \int_0^t \left[\left(\sum_{a=1}^z \Delta f_a \right)^2 + (\Delta P_{tie})^2 \right] . dt \quad (17)$$

$$FF = IAE = \int_0^t \left[\sum_{a=1}^z |\Delta f_a| + |\Delta P_{tie}| \right] .dt \quad (18)$$

$$FF = ITAE = \int_0^t \left[\sum_{a=1}^z |\Delta f_a| + |\Delta P_{tie}| \right] .t.dt \quad (19)$$

where Δf_a represents the frequency deviation for area number a , ΔP_{tie} represents the tie-line power deviation, t represents the total simulation time of over which the power system is operated.

From the literature review, the ITAE-optimized controllers are desired in LFC systems. Thus, in this paper, a novel weighted goal method based on the ITAE performance criterion was designed and implemented. This method is used as the fitness function for tuning the parameters of the 2DOF-ID controller.

4.2. Proposed Integral-Based Weighted Goal Fitness Function (IB-WGFF)

In this paper, two objective performance criteria are proposed to be the fitness function used with the DA explained in Section 3 to design the 2DOF-PID modelled in Section 2.1 and indicated by Equation 8. The first objective is to minimize the integrated time-weighted absolute frequency deviations of the two-area power system (Δf_1 and Δf_2). The second objective is to minimize the integrated time-weighted absolute power deviation (ΔP). The two objectives are combined as a single objective with weighting coefficients C_1 and C_2 . This control objective will make the dynamic response of the power system more robust under variable loads and uncertainties in power system parameters.

Equation (20) shows the mathematical design of the proposed Integral-Based-weighted Goal Fitness Function (IB-WGFF) to be optimized using the DA algorithm for regulating the power and frequency fluctuations of a two-area interconnected power system. The fitness/objective function (FF) to be optimized is a weighted goal type of integral performance over the simulation time (50 s). To approve the performance of the proposed IB-WGFF under various performance criteria, the corresponding values of ITSE, ISE, ITAE and the IAE will also be implemented and calculated.

$$FF = IB - WGFF = C_1 \left[\int_0^t \left(\sum_{a=1}^z |\Delta f_a| \right) t.dt \right] + C_2 \left[\int_0^t |\Delta P_{tie}| .t.dt \right] \quad (20)$$

where a is the number of interconnected area in the electrical power system; $\sum_{a=1}^z |\Delta f_a| = \Delta f_1 + \Delta f_2$; Δf_1 is the frequency deviation of area1; Δf_2 is the frequency deviation for are2 of two-area interconnected power system; t is the total simulation time; C_1 and C_2 represents

the weighting coefficients of the proposed fitness function. The parameters C_1 and C_2 are assumed to be in the range between $[0, 1]$ such that $C_1 + C_2 = 1$. Increasing C_1 and decreasing C_2 in at same time makes the frequency deviation (Δf_d) responses better while increasing C_1 and decreasing C_2 makes the tie-line power dynamic's response smoother and better. Varying C_1 and C_2 will affect the power system dynamic, and this effect will be investigated later in Section 5.2.

The main procedure of the DA using the proposed IB-WGFF, modelled in Equation (20) for optimizing the parameters of the suggested 2-DOF-PID control scheme, is shown in Figure 3. The upper (U) and the lower (L) control limits used for the control parameters are defined as shown in Equation (19).

$$\begin{aligned} K_p^L &\leq K_{p1}; K_{p2} \leq K_p^U \\ K_i^L &\leq K_{i1}; K_{i2} \leq K_i^U \\ K_d^L &\leq K_{d1}; K_{d2} \leq K_d^U \\ PW^L &\leq PW_1; PW_2 \leq PW^U \\ DW^L &\leq DW_1; DW_2 \leq DW^U \end{aligned} \quad (21)$$

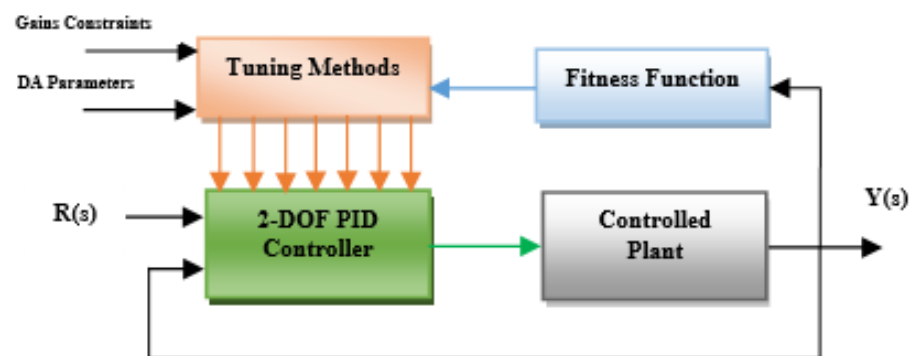


Figure 3. Tuning process of the parameters using IB-WGFF.

The lower values of the control parameters (K_p^L , K_i^L , and K_d^L) are chosen to be a value of zero, and their upper (K_p^U , K_i^U , and K_d^U) values are chosen to be a value of 1. The lower limits of (PW^L , DW^L) are chosen to be zero whereas their upper limits (PW^U , DW^U) are set to a value of 2.

4.3. Implementation of the Proposed DA-2DOF-PID Controller

The proposed 2DOF-PID control scheme is implemented in MATLAB software using 2017b operated on Intel core i5 2.3 GHz processor PC. Equation (20) represents the proposed IB-WGFF that is solved using the DA to control and improve the power/frequency of the two-area interconnected power systems. Equations (16)–(19) represent the Fitness/Objective functions in the literature used to compare and prove the effectiveness of the proposed 2DOF-PID control scheme. The implemented DA's flow chart is displayed in Figure 4. According to many trials, the DA's parameters implemented in the optimization process are indicated in Table 2. The DA has been run for 15 independent trials using different settings till the solutions are tangible close to each other.

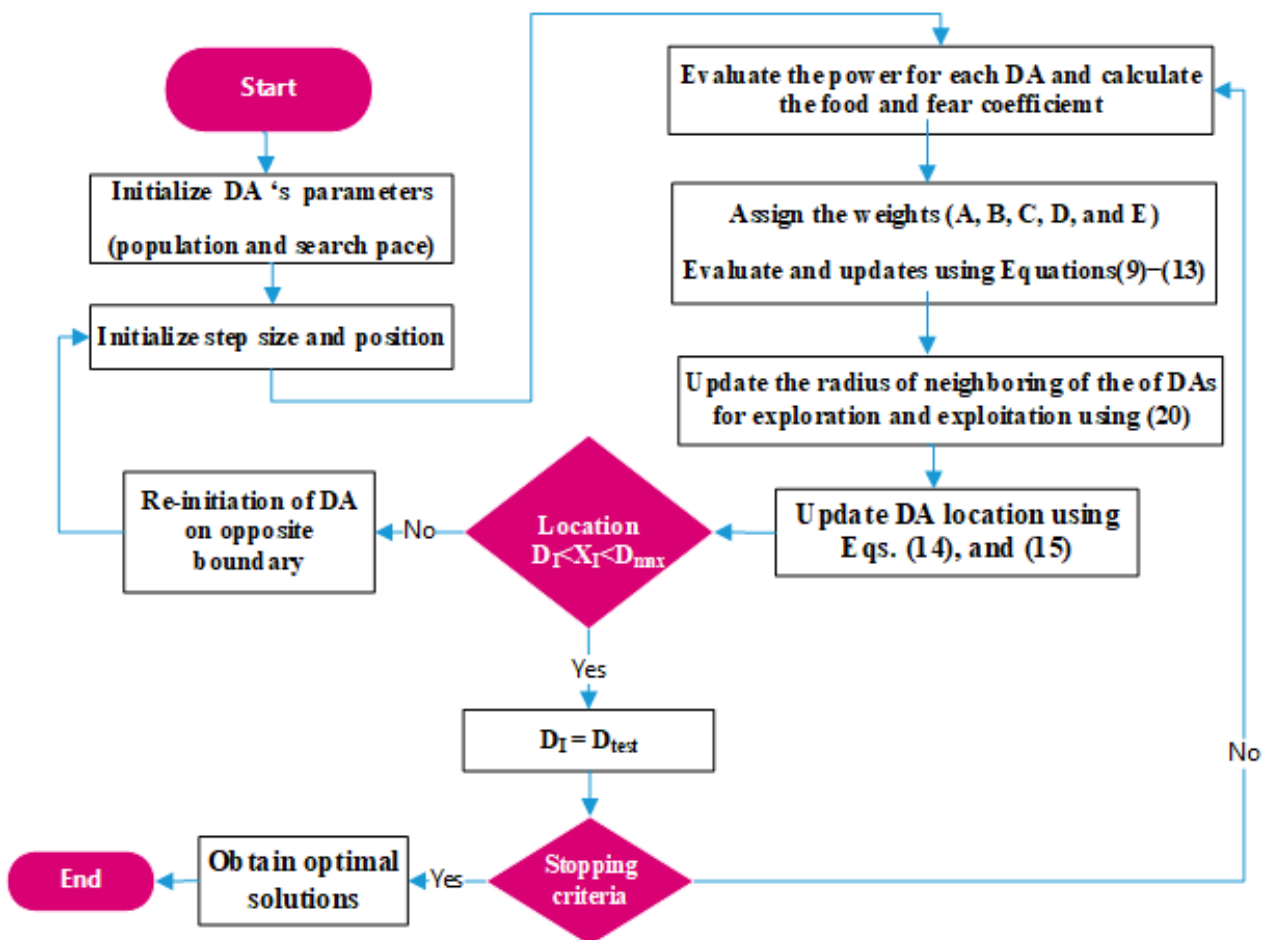


Figure 4. Dragonfly Algorithm (DA) Implementation.

Table 2. DA's parameters.

Parameters	Values
Population Size	50
Number of iterations	30
<i>A</i> , Separation weighted coefficients,	0.25
<i>B</i> , Alignment weighted coefficients	0.15
<i>C</i> , Cohesion weighted coefficients	0.96
<i>D</i> , Food weighted coefficients	0.6
<i>E</i> , is the enemy factor	1
ω , inertial weighted coefficient	[0.25, 95]

4.4. Implementation of the GA-2DOF-PID Controller

In this paper, the GA-2DOF-PID controller is assumed for comparison. The parameters of the 2DOF-PID-controller are tuned by GA using the proposed IB-WGFF indicated in Equation (18) and the performance criteria in the literature which indicated in Equations (14)–(17). The initial population size of chromosomes that signifies the 2DOF-PIDb controller parameter is randomly generated. Then, the chromosomes are calculated according to the selected fitness/objective function defined by Equations (14)–(18) is Sections 4.1 and 4.2. A new population that is based on the fitness/objective of individuals is selected. Genetic mutation and crossover are implemented in members of the population

for creating the new solutions. The process of creation and evaluation the new population is continued until termination criteria has been satisfied [36,37]. According to experience, mutation should be completed with a low probability that ranges from 0.1 to 2%, whereas crossover should be between 60 to 90%. The GA has been run for 15 independent trials using different settings till the solutions are tangible close to each other. Again, the DA-2DOF-PID controllers are compared with the 2DOF-PID controllers tuned by GA as discussed in [37]. According to trials, the basic parameters of GA are given in Table 3. The DA-2DOF-PID controllers are also compared to the classical 2DOF-PID controller.

Table 3. GA Parameters.

Parameters	Values
population size	50
Number of generations	30
Acceleration constant, C_1	0.5
Acceleration constant, C_2	1.5
Initial inertia weight, w_{max}	0.9
Final inertia weight, w_{min}	0.4

5. Results and Discussion

This section is dedicated for investigating the performance of the proposed control scheme in controlling and suppressing the frequency/power in a two-area interconnected power system. In this section, the parameters of the proposed 2DOF-PID are designed under the conditions of a step dynamic load implemented at the time instant 5 s. Five parts are designed and investigated in this section of the paper. The first part introduces the design of the 2DOF-PID controller using the classic method (i.e., the Z-N tuning method). The second parts introduce design and investigation of the 2DOF-PID scheme using DA via the new IB-WGFF indicated in Equation (20). Section three is designed to investigate the controlled system dynamic using the DA via the Fitness/objective functions used in the literature and indicated by Equations (16)–(19). The fourth section introduces a comparison between the proposed control scheme and other methods used in the literature. Finally, the fifth section introduces a comparison with the results obtained using the GA. The complete model using MATLAB Simulink of the two-area power system with the 2DOF PID controllers is shown in Figure 5.

5.1. System Dynamic using 2-DOF-PID Controllers Tuned Conventionally

In this sub-section, the two-area power system shown in Figure 5 is used to investigate the frequency and power deviations. In this system, each area encompasses a speed governor, steam turbine, and generator of 2000 MW rating, and a nominal step load of 2000 MW applied at the time instant 5 s. The ZN tuning method used to design the parameters of the 2DOF-PID-controller is completed using the MATLAB[®] toolbox software (R2021a). The classical design method is supposed for optimizing the 2DOF-PID controller under a normal step load of 1 pu. is applied at the time instant of 5 s. The parameters of the 2DOF-PID controllers, using Z-N method, and the dynamic response parameters of the controlled two-area interconnected power system are demonstrated in Table 4. Figures 6 and 7 indicate the frequency deviation (Δf_1) for area 1, frequency deviation (Δf_2) for area 2 of the controlled interconnected power system, respectively. Figure 8 demonstrates the power deviation (ΔP) of the system using conventional 2FOPID controller.

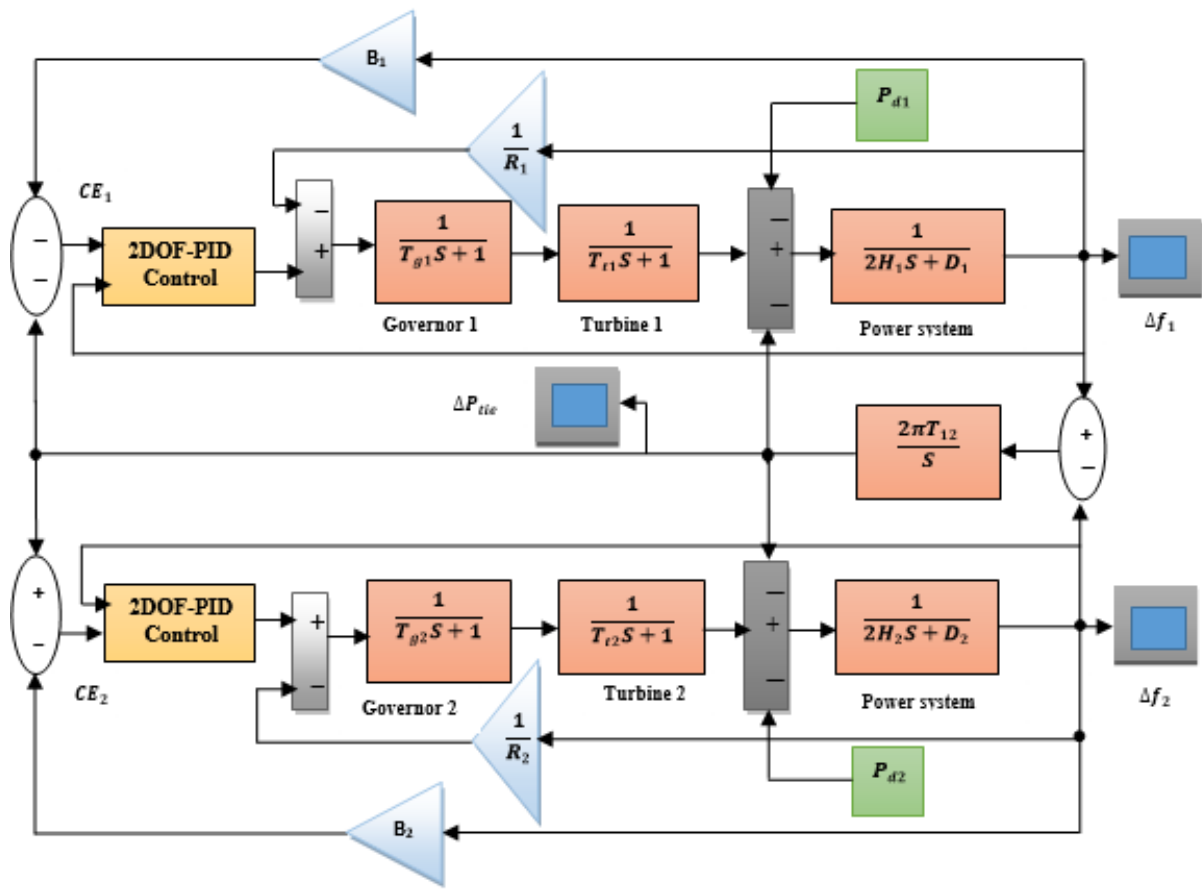


Figure 5. Complete SIMULINK model for the two-area power system.

Table 4. Efforts implementing conventional-FOPID controller.

FO-PID Parameters	K_P	K_I	K_D	PW	DW	Seeking Time
Area 1	0.9213	0.7024	0.8312	0.9034	0.4434	Very large time
Area 2	0.8324	0.7034	0.5354	0.6015	0.6415	

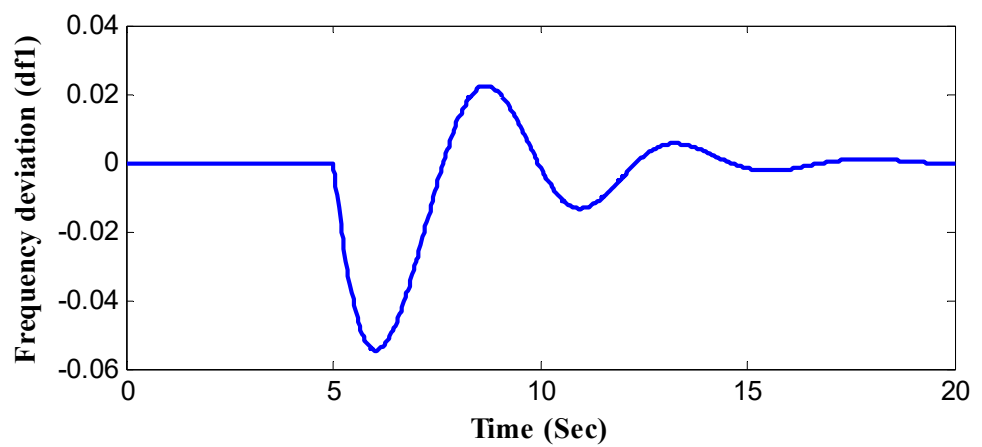


Figure 6. Frequency deviation (Δf_1) using conventional 2DOF-OPID controller.

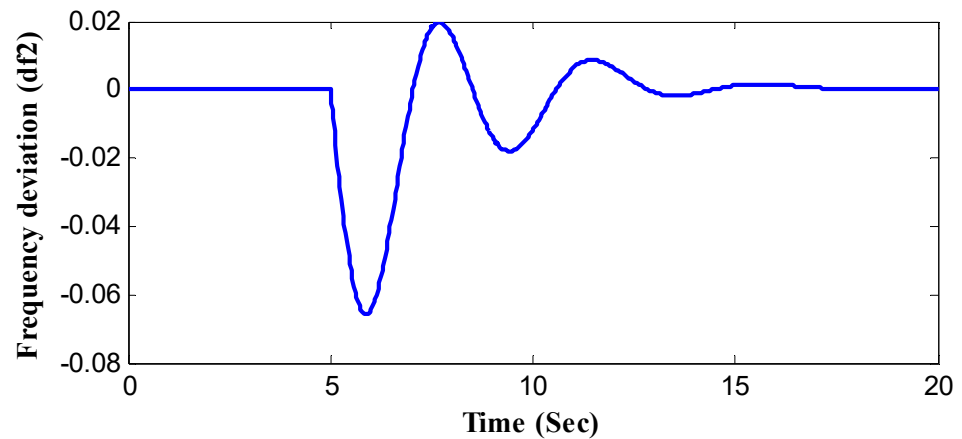


Figure 7. Frequency deviation (Δf_2) using conventional 2DOF-OPID controller.

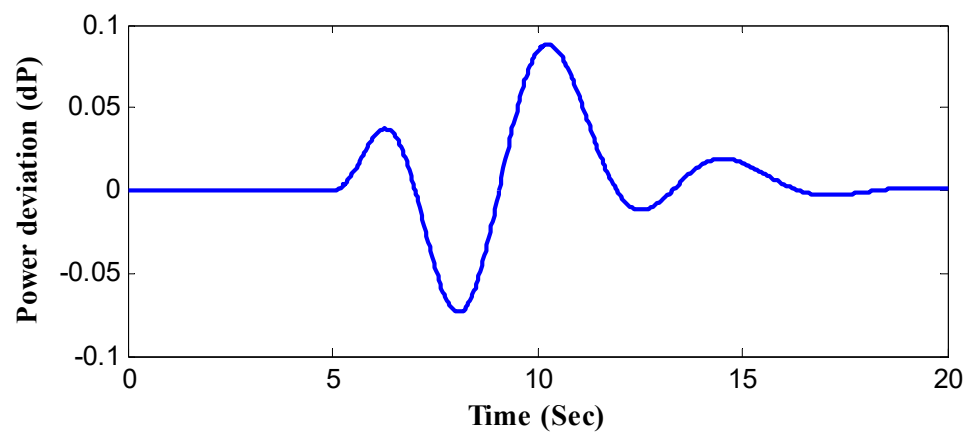


Figure 8. Tie-line Power deviation (ΔP) using conventional 2DOF-PID controller.

It is evident from Figures 6 and 7 that the two area have oscillating frequency over a large period of time besides the multiple and large values of undershoots, thus the parameters of the 2DOF-PID controllers still need to be accurately tuned using high performance objectives and approaches. It is evident also from Figure 8 that the power deviation has multiple and very large overshoots and long settling time and therefore, the parameters of the controllers have to be optimized using powerful approach.

5.2. Results using DA with the Proposed IB-WGFF

In this sub-section of the simulation results, the parameters of the 2DOF-PID control scheme, under step load disturbance at the time instant 5 s, are designed using the DA via the proposed IB-WGFF indicated in Equation (20). The proposed IB-WGFF is implemented by trying various weighting coefficient C_1 and C_2 such that C_1 and C_2 are between $[0, 1]$ and $C_1 + C_2 = 1$. The efforts of the two-area inter-connected power system, shown in Figure 5, optimized using the DA via the proposed IB-WGFF, are shown in Table 4. The time responses of the frequency deviations (i.e., Δf_1 and Δf_2) for the two areas and the tie-line power deviation (ΔP) are shown in Figures 9–11, respectively.

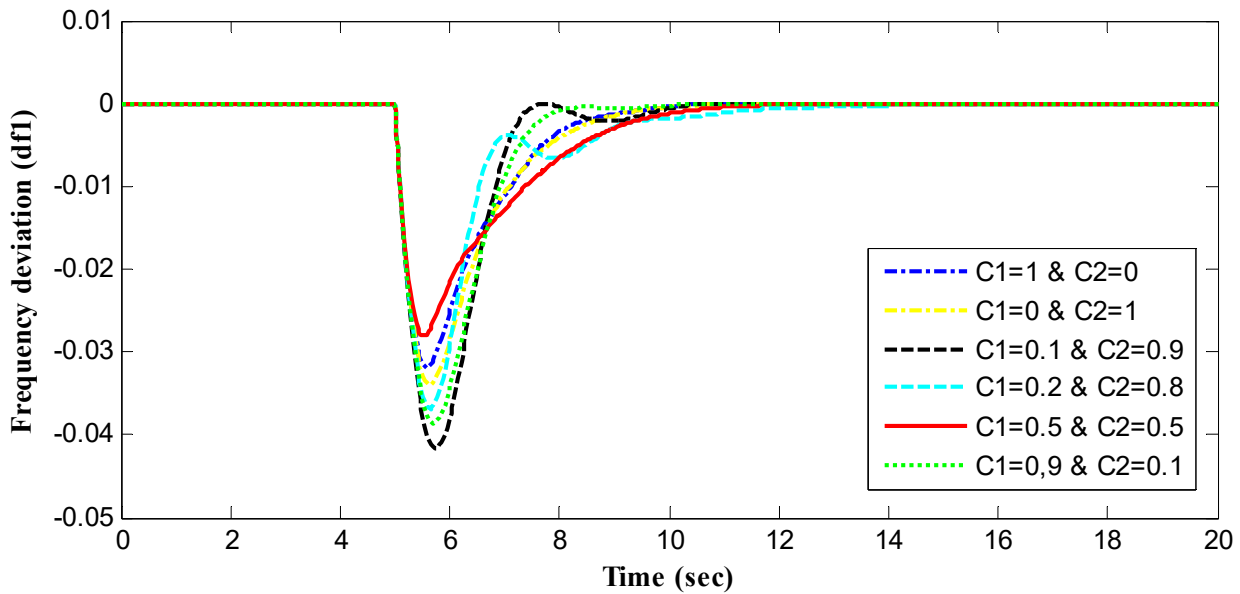


Figure 9. Frequency deviation Δf_1 for area1 using the proposed IB-WGFF.

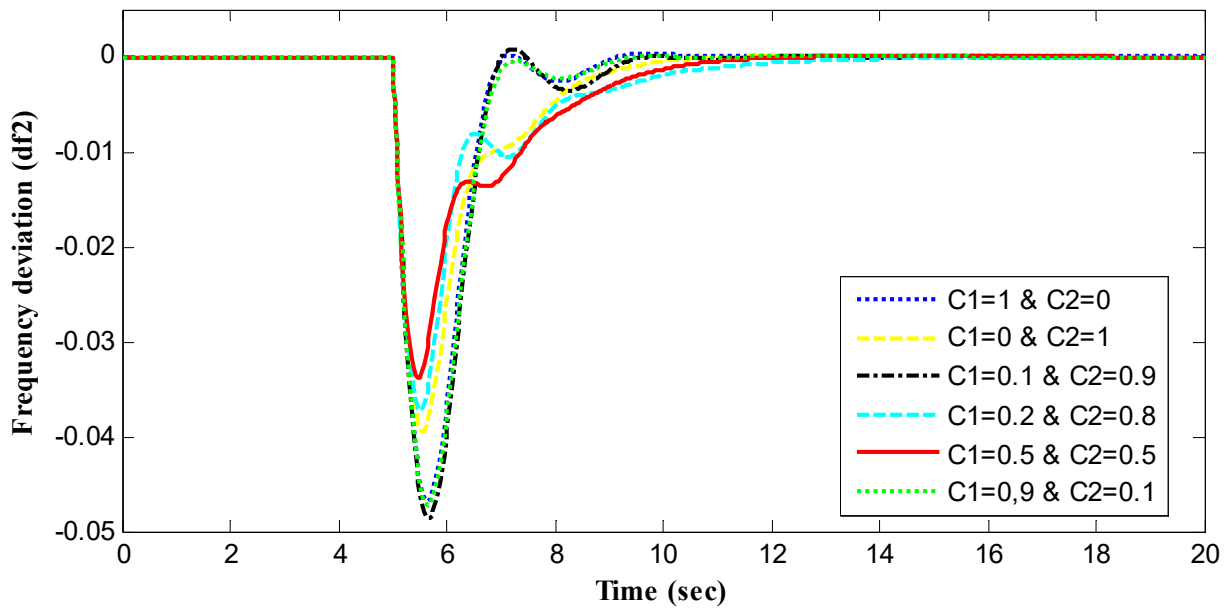


Figure 10. Frequency deviation Δf_2 for area 2 using the proposed IB-WGFF.

From Figures 9 and 10 and Table 4, it is evident that the frequency deviation responses (i.e., Δf_1 and Δf_2) of the controlled power system are improved with varying the weighting coefficients C_1 and C_2 . In addition, it is concluded from Table 5 and Figure 11 that the time-response of the tie-line power deviation (ΔP) is improved. It is evident that the dynamic response of the controlled power system is improved in all cases denoted in Table 5. Figures 9–11 and Table 5 show that the frequency and power deviations have optimum values using the proposed IB-WGFF in case of ($C_1 = 0.5$ and $C_2 = 0.5$). According to the priority, the designer engineer will select between different cases demonstrated in Table 5.

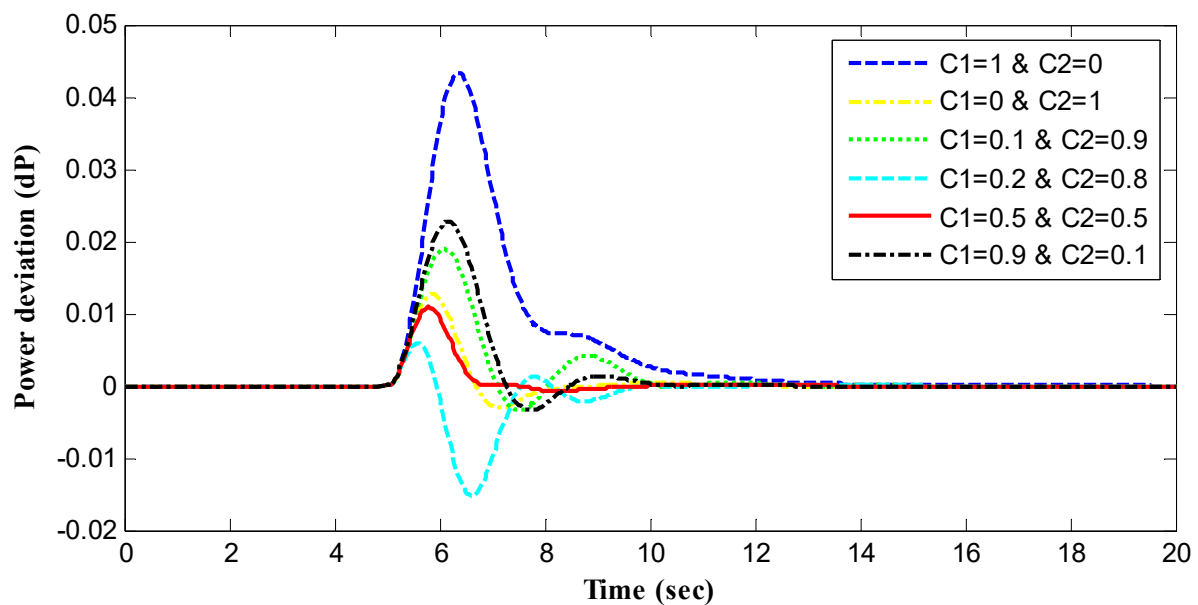


Figure 11. Power deviation ΔP using the proposed IB-WGFF.

Table 5. System efforts using DA-FOPID controller via the proposed IB-WGFF.

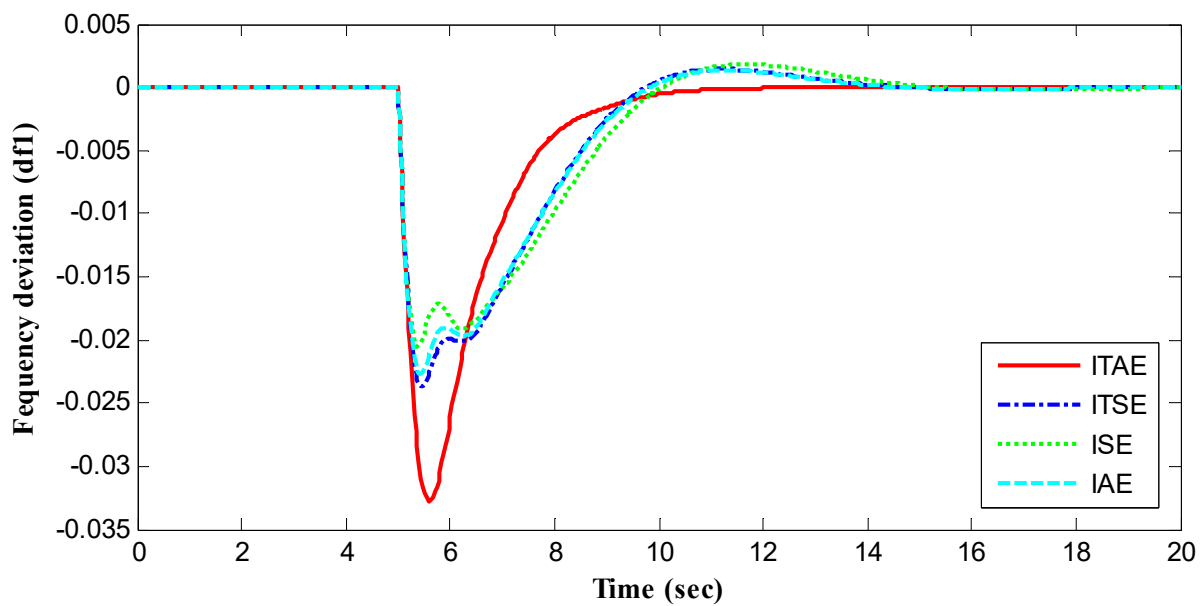
Parameters	2-DOF PID Controller (AREA 1)					2-DOF PID Controller (AREA 2)					Fitness Function
	C_1 and C_2	K_p	K_i	K_d	PW	DW	K_p	K_i	K_d	PW	DW
0 and 1	1.0000	0.8624	0.6317	1.7320	1.1800	0.7505	1.0000	0.6840	1.6648	1.7315	0.106046
0.1 and 0.9	1.0000	0.8528	0.4163	1.5577	1.0554	0.6907	0.9610	0.5588	1.4008	1.2963	0.250180
0.2 and 0.8	1.0000	0.8291	0.2698	2.0000	2.0000	1.0000	1.0000	0.6349	1.7490	2.0000	0.262111
0.3 and 0.7	1.0000	0.8614	0.8169	2.0000	1.3534	0.9115	1.0000	0.83141	1.70759	2.0000	0.278407
0.4 and 0.6	1.0000	0.8712	0.4138	1.9143	1.5160	0.7819	1.0000	0.9755	1.8252	1.0090	0.352105
0.5 and 0.5	1.0000	0.8680	0.9555	1.8034	0.8308	1.0000	1.0000	0.6134	1.2911	2.0000	0.399303
0.6 and 0.4	0.9910	0.8759	0.4285	1.7924	1.4968	0.8316	1.0000	0.8726	1.4925	1.0982	0.465029
0.7 and 0.3	0.7733	0.8765	0.2956	2.0000	1.6655	0.6831	1.0000	1.0000	1.4374	0.8161	0.517983
0.8 and 0.2	1.0000	1.0000	0.80587	2.0000	1.1101	0.88687	1.0000	0.5545	1.1164	1.4286	0.625108
0.9 and 0.1	0.8448	0.8920	0.7857	1.8841	0.6918	0.8434	1.0000	0.6676	1.1299	1.1732	0.609655
1 and 0	1.0000	1.000	0.6936	2.0000	1.1717	0.8781	1.0000	0.5342	1.1930	1.4938	0.641395

5.3. Results Implementing Different Performance Indices in Literature

In this sub-section of the article, the parameters of the 2FOF-PID controller is designed using the DA via the performance indices in the literature indicated by Equations (16)–(19). The parameters of the upper and lower boundaries of the 2DOF-PID controller are the same as mentioned previously in Section 4.2. The main variable parameters of the DA are set the same as indicated in Table 2. The DA has been run for 15 independent trials using different settings till the solutions are tangible close to each other. Table 6 demonstrates the efforts of the 2DOF-PID controllers optimized using DA via the ITAE, ITSE, IAE, and ISE used in the literature. The frequency deviations for the two-areas (i.e., Δf_1 and Δf_2) obtained by DA-2DOF-PID via the various fitness are indicated in Figures 12 and 13. The tie-line power deviation (ΔP) is indicated in Figure 14.

Table 6. Efforts of different performance criteria in the literature.

Response and PID Parameters		ITAE	ITSE	IAE	ISE
Area 1	K_P	0.96642	1.00000	1.00000	1.00000
	K_I	0.93701	0.96773	1.00000	0.94818
	K_D	0.79796	0.82892	0.98677	1.00000
	PW	2.00000	1.94039	2.00000	2.00000
	DW	0.95602	1.86494	1.68953	2.00000
Area 2	K_P	0.70693	0.87803	0.73250	1.00000
	K_I	0.6000	1.00000	1.00000	0.95282
	K_D	0.78672	1.00000	1.00000	0.81901
	PW	1.64358	1.15338	1.49248	1.06404
	DW	1.09507	1.33994	1.34948	2.00000
FF Val.		0.35286	0.00751	0.04615	0.00100
Seeking Time		345.105	347.8026	325.40	310.12

**Figure 12.** Frequency deviation Δf_1 for area 1 using performance objectives in the literature.

It is evident from Figures 12 and 13 that the frequency deviation of the two-area (i.e., Δf_1 and Δf_2) implementing the ITAE is the smoothest and the best in overshoot, and settling time but, it has larger undershoot compared with the other performance indices. It is evident from Figure 14 that the 2DOF-PID optimized using DA via the ITAE shows the lowest overshoot, undershoot, and settling time in case of the tie-line power.

5.4. Comparison with Different Controllers

To emphasize the superiority of the proposed 2DOF-PID optimized using DA via the proposed IB-WGFF indicated in Equation (20), the obtained results are compared with the results obtained using the conventional 2DOF-PID and the 2DOF-PID optimized using DA via the best performance criterion implemented in the literature and indicated in Equations (16)–(19). For a fair comparison, the DA has been run for 15 independent trials using different settings till the solutions are tangible and close to each other in each case. The same parameters and constraints indicated and discussed in Sections 4.2 and 4.4

are used to design the 2DOF-PID control scheme via the different fitness functions. For the conventional 2-DOF-PID, the classical design method is applied for optimizing its parameters as discussed in Section 5.1. The same trials are implemented in the tuning process of the conventional 2DOF-PID controller.

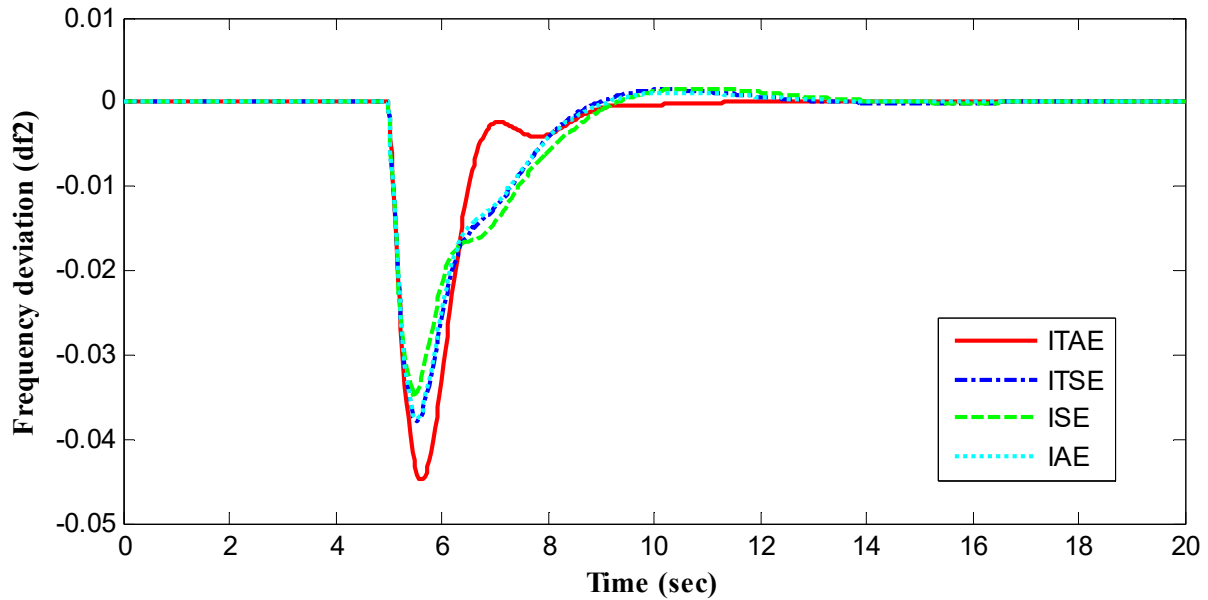


Figure 13. Frequency deviation Δf_2 implementing performance objectives used in the literature.

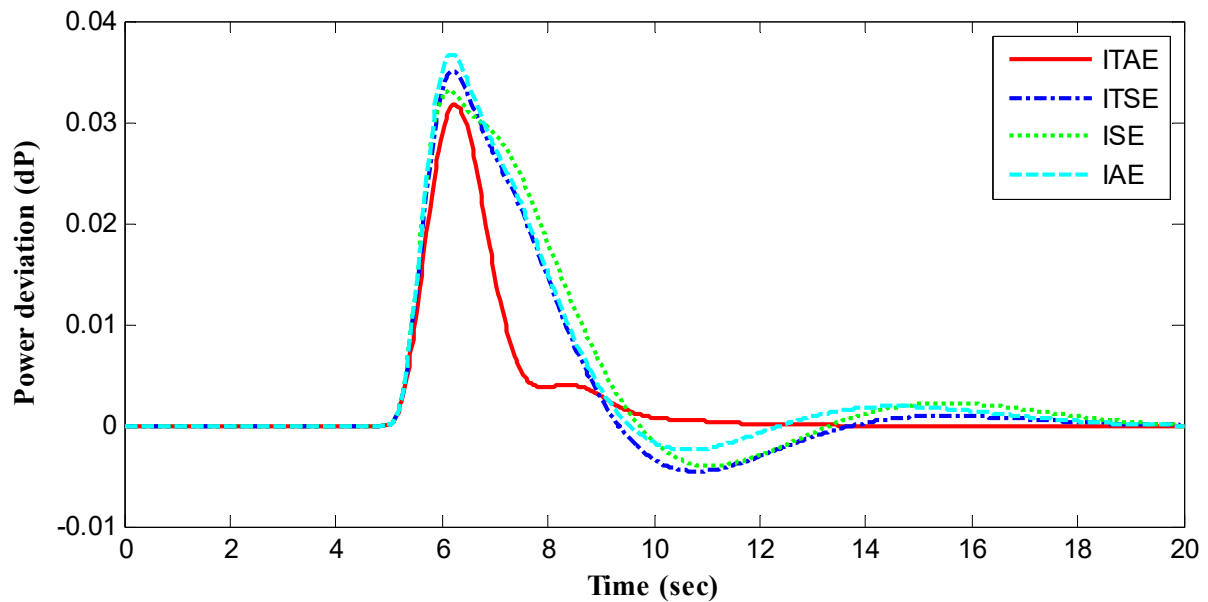


Figure 14. Power deviation ΔP using performance indices used in the literature.

The parameters of the 2DOF-PID control scheme optimized conventionally, using the DA via the ITAE, using the DA via the proposed IB-WGFF are indicated in Table 7. In addition, the dynamic responses of the frequency deviations for the two-areas (i.e., Δf_1 and Δf_2) and the tie-line power deviation (ΔP) for the conventional 2DOF-PID, the DA-2DOF-PID using the ITAE, and the DA-2-DOF-PID controller via the proposed IB-WGFF (for $C_1 = 0.5$ and $C_2 = 0.5$) are shown in Figures 15–17.

Table 7. Efforts using conventional 2-DOF-PID, DA-2-DOF-PID-ITAE, and DA-2-DOF-PID-IB-WGFF.

Response and PID Parameters	ITAE		Conventional		Proposed IB-WGFF	
	Area 1	Area 2	Area 1	Area 2	Area 1	Area 2
K_P	0.96642	0.70693	0.92134	0.82245	1.0000	1.0000
K_I	0.93701	1.00000	0.70024	0.73345	0.8680	1.0000
K_D	0.79796	0.78672	0.83123	0.50543	0.9555	0.6134
PW	2.00000	1.64358	0.9034	0.60156	1.8034	1.2911
DW	0.95602	1.09507	0.44345	0.64156	0.8308	2.0000
FF. Value	0.35286				0.399303	
Seeking Time	345.105		Very large time		343.261	
Overshoot	Δf_1	0.0000	0.0235		0.0	
	Δf_2	0.0000	0.020		0.0	
	ΔP	0.0328	0.092		0.0153	
Undershoot	Δf_1	0.0355	0.0545		0.0241	
	Δf_2	0.0453	0.0665		0.0321	
	ΔP	0.0000	0.074		0.0000	
S.S. Error	Δf_1	6.57×10^{-6}	344×10^{-6}		1.931×10^{-6}	
	Δf_2	29.99×10^{-6}	131×10^{-6}		3.143×10^{-6}	
	ΔP	18.34×10^{-6}	1059×10^{-6}		4.5682×10^{-6}	
Settling Time (Sec.)	Δf_1	7.42	11.52		6.571	
	Δf_2	6.83	9.43		6.731	
	ΔP	3.724	12.45		1.543	

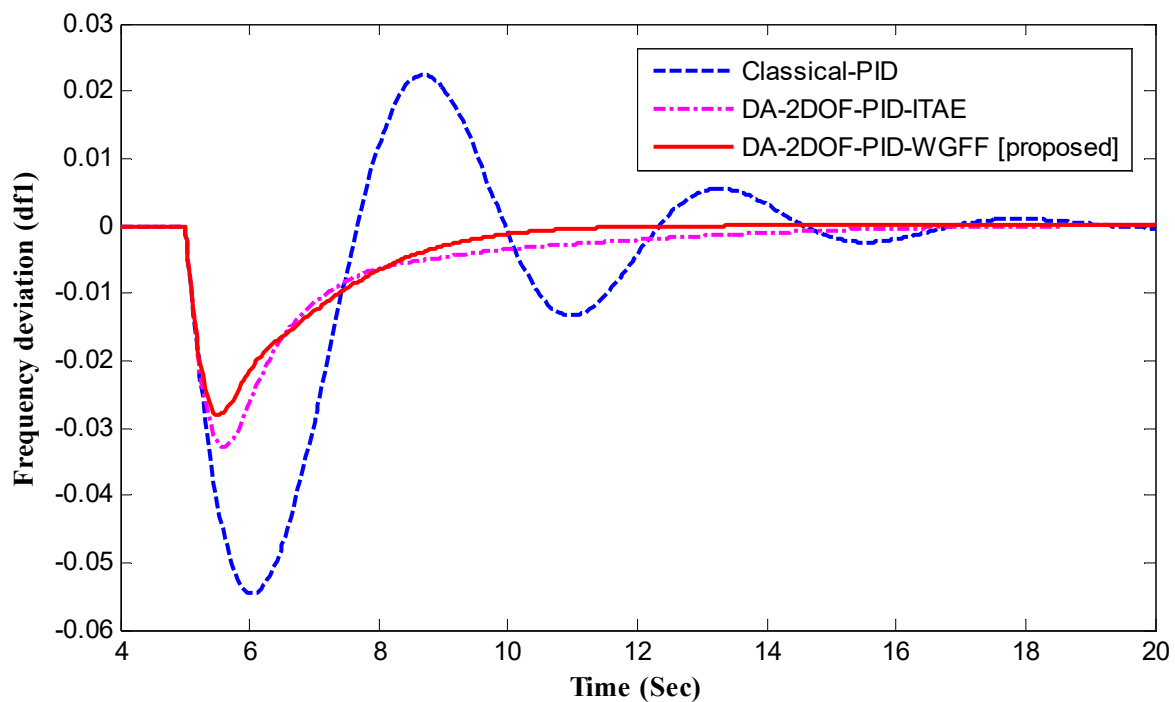


Figure 15. Δf_1 using the proposed 2DOF-PID controller compared with other controllers.

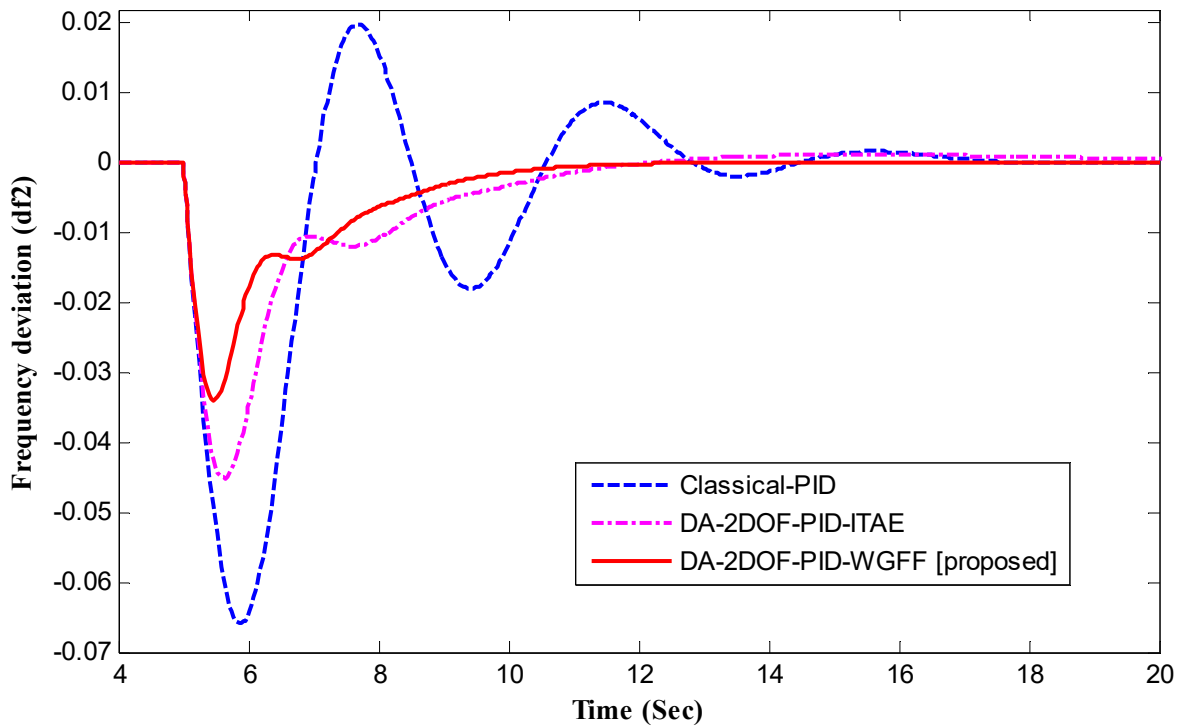


Figure 16. Δf_2 using the proposed 2DOF-PID controller compared with other controllers.

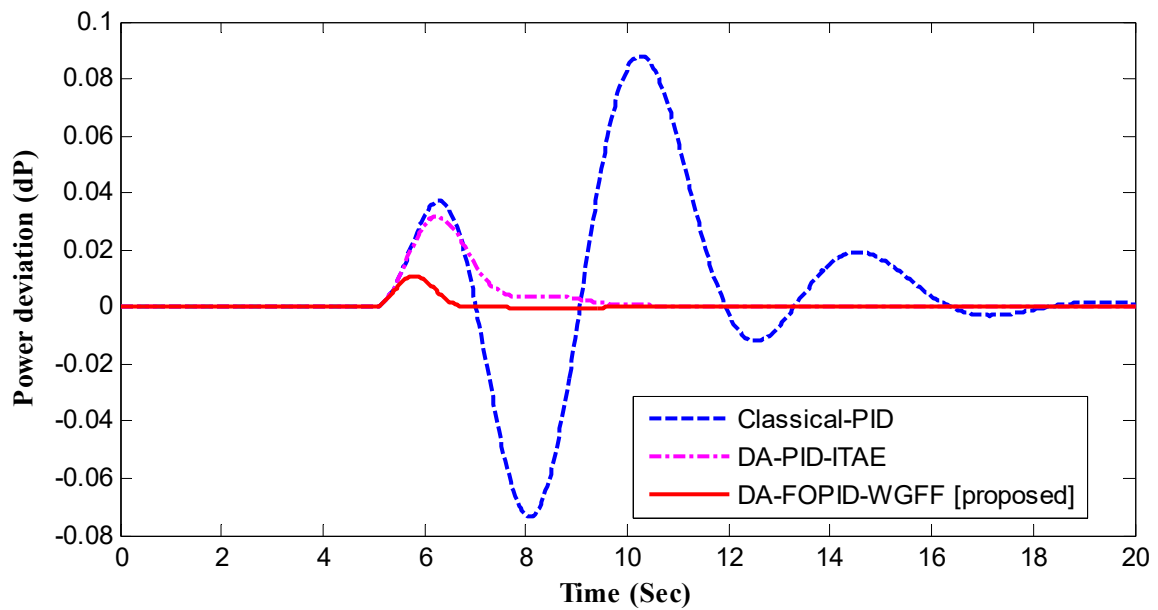


Figure 17. ΔP using the proposed 2DOF-PID controller compared with other controllers.

It is obvious, from Table 7 and Figures 15–17, that the frequency deviation of the two-area (i.e., Δf_1 and Δf_2) and the tie-line power deviation (ΔP) of the proposed 2DOF-PID controller is the smoothest and the best in overshoot, undershoot, and settling time. The conventional 2DOF-PID shows larger undershoots and overshoots, and the performance of the conventional 2DOF-PID controller is worse than the DA-2DOF-PID-ITAE and the proposed 2DOF-PID controller. It is concluded, from the comparison, that the 2DOF-PID controller tuned using DA via proposed IB-WGFF (for $C_1 = 0.5$ and $C_2 = 0.5$) has been verified to be the best control scheme.

5.5. Comparison with GA

In this sub-section of the results, the advantage of the proposed 2DOF-PID control scheme optimized using DA via the IB-WGFF indicated in Equation (20) is emphasized in terms of performance. The GA in [37] with the parameters indicated and discussed in Sections 4.2 and 4.4 is used to design the 2DOF-PID control scheme. The obtained results are compared with those obtained by the proposed 2DOF-PID control scheme and the classical 2DOF-PID controller.

The efforts of the system under study and the parameters of the 2DOF-PID controllers are shown in Table 8. Figures 18–20 show the frequency deviations Δf_1 , Δf_2 , and power deviation (ΔP) of the system, respectively, using GA-2DOF-PID-ITAE, GA-2DOF-PID-IB-WGFF, and the classical 2DOF-PID. Figures 21–23 show the frequency deviations (Δf_1 , Δf_2) and power deviation (ΔP) of the system, respectively, using GA with the ITAE. Figures 24–26 show the frequency deviations (Δf_1 , Δf_2) and power deviation (ΔP) of the system, respectively, using the GA and DA with the ITAE. Figures 27–29 show the frequency deviations (Δf_1 , Δf_2) and power deviation (ΔP) of the system, respectively, using GA with the proposed IB-WGFF.

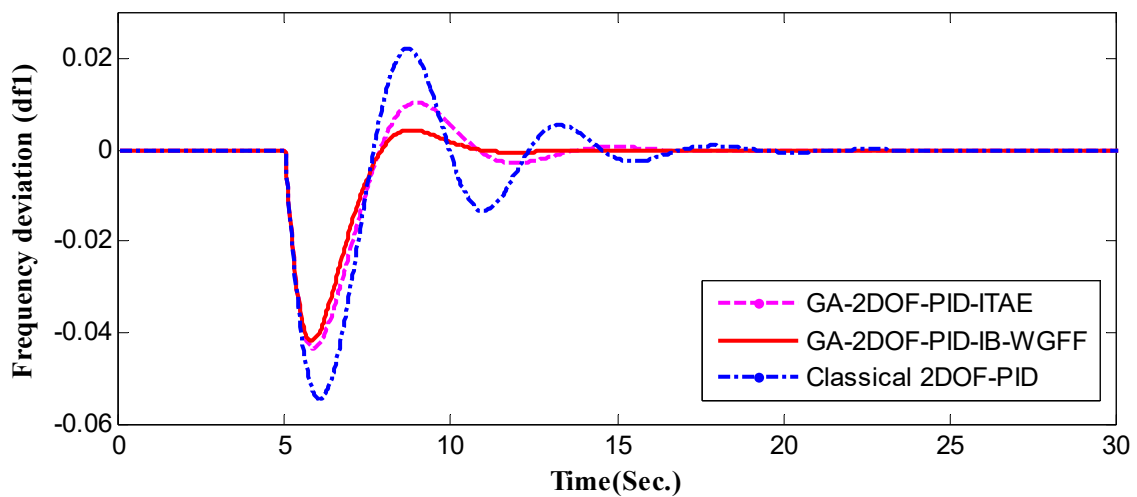


Figure 18. Δf_1 , using GA implementing ITAE, IB-WGFF and classical 2DOF-PID.

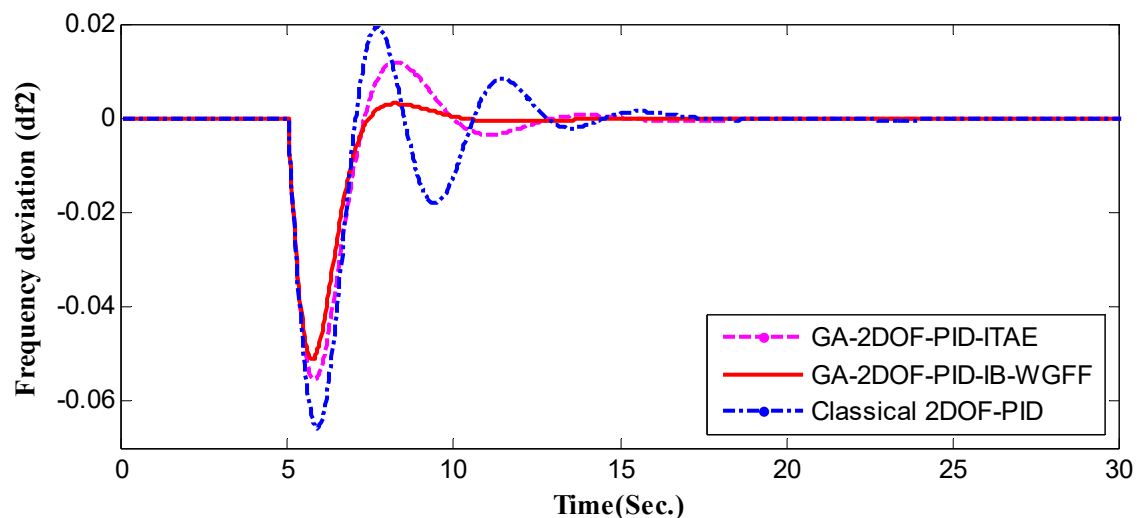


Figure 19. Δf_2 , using GA implementing ITAE, IB-WGFF and classical 2DOF-PID.

Table 8. Efforts using conventional 2DOF-PID, DA-2DOF-PID-ITAE, and GA-2DOF-PID-ITAE, and DA-2DOF-PID-IB-WGFF.

Response and PID Parameters	Technique	ITAE		Proposed IB-WGO		Conventional	
		Area 1	Area 2	Area 1	Area 2	Area 1	Area 2
K_P	GA	0.72699	0.27871	0.83946	0.762206	0.92134	0.82245
	DA	0.96642	0.70693	1.0000	1.0000		
K_I	GA	0.83020	0.94735	0.80700	0.92890	0.70024	0.73345
	DA	0.93701	1.00000	0.8680	1.0000		
K_D	GA	0.60058	0.39374	0.72354	0.80695	0.83123	0.50543
	DA	0.79796	0.78672	0.9555	0.6134		
PW	GA	1.45231	1.168094	1.46078	0.71085	0.9034	0.60156
	DA	2.00000	1.64358	1.8034	1.2911		
DW	GA	0.90314	1.63051	0.72796	0.88071	0.44345	0.64156
	DA	0.95602	1.09507	0.8308	2.0000		
FF. Value	GA	0.738761		0.657643			
	DA	0.352865		0.399303			
Seeking Time	GA	445.234		442.343		Very large time	
	DA	345.105		343.261			
Overshoot	Δf_1	GA	0.0153		0.0083		0.0235
		DA	0.0000		0.000		
	Δf_2	GA	0.0178		0.0073		0.020
		DA	0.0000		0.000		
	ΔP	GA	0.0435		0.0273		0.092
		DA	0.0328		0.0153		
Undershoot	Δf_1	GA	0.0493		0.0412		0.0545
		DA	0.0355		0.0244		
	Δf_2	GA	0.0545		0.048		0.0665
		DA	0.0453		0.0321		
	ΔP	GA	0.0321		0.0234		0.074
		DA	0.0000		0.000		
S.S. Error	Δf_1	GA	45.372×10^{-6}		9.16×10^{-6}		344×10^{-6}
		DA	6.57×10^{-6}		1.931×10^{-6}		
	Δf_2	GA	86.31×10^{-6}		32.78×10^{-6}		131×10^{-6}
		DA	29.99×10^{-6}		3.143×10^{-6}		
	ΔP	GA	35.34×10^{-6}		15.856×10^{-6}		1059×10^{-6}
		DA	18.34×10^{-6}		4.5682×10^{-6}		
Settling Time (Sec.)	Δf_1	GA	9.343		6.312		11.52
		DA	7.423		6.571		
	Δf_2	GA	9.843		6.233		9.43
		DA	6.832		6.731		
	ΔP	GA	7.576		7.322		12.45
		DA	3.724		1.543		

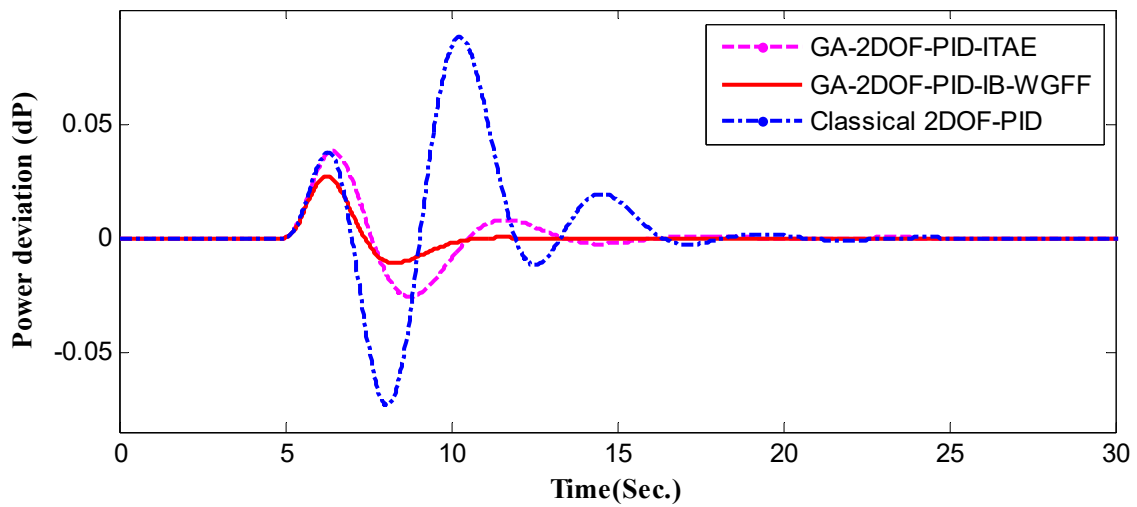


Figure 20. ΔP using GA using GA implementing ITAE, IB-WGFF and classical 2DOF-PID.

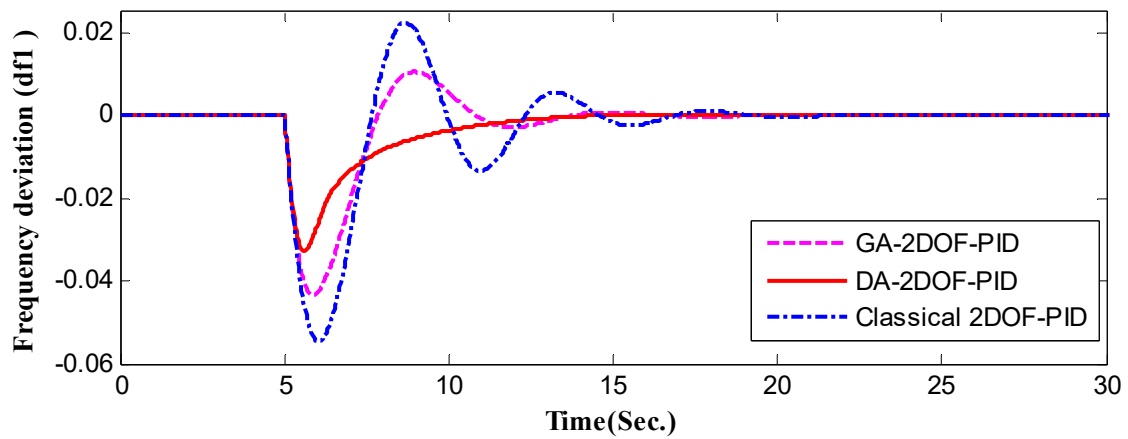


Figure 21. Δf_1 , using GA-2DOF-PID, DA-2DOF-PID, and classical-2DOF-PID with ITAE.

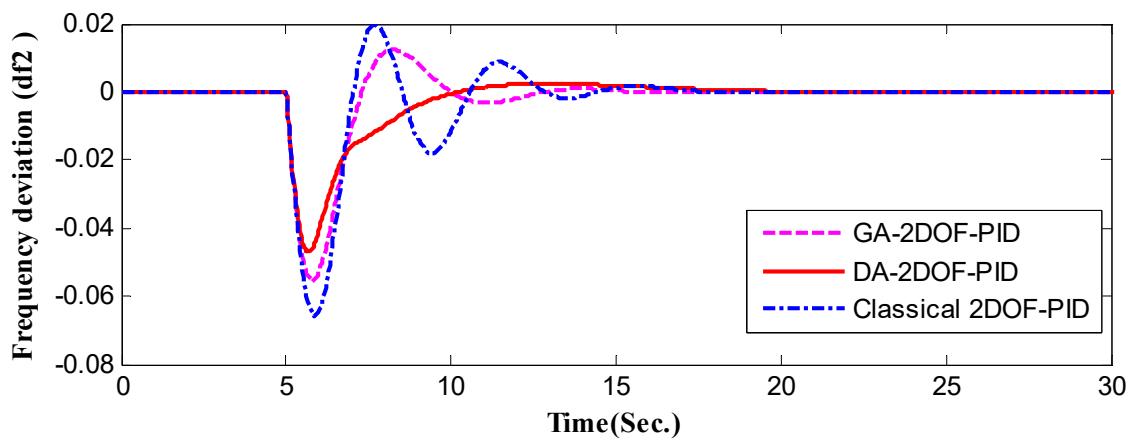


Figure 22. Δf_2 , using GA-2DOF-PID, DA-2DOF-PID, and classical-2DOF-PID with ITAE.

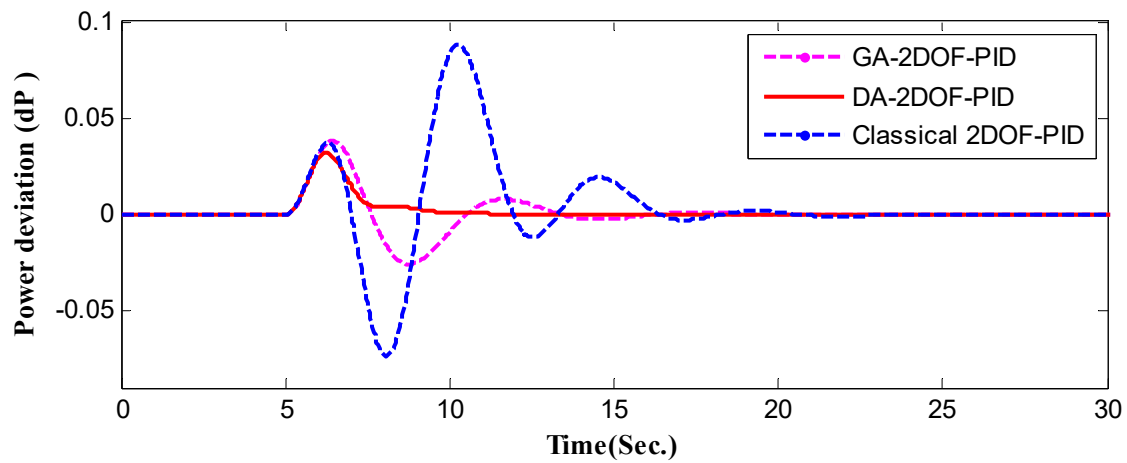


Figure 23. ΔP using GA-2DOF-PID, DA-2DOF-PID, and classical-2DOF-PID with ITAE.

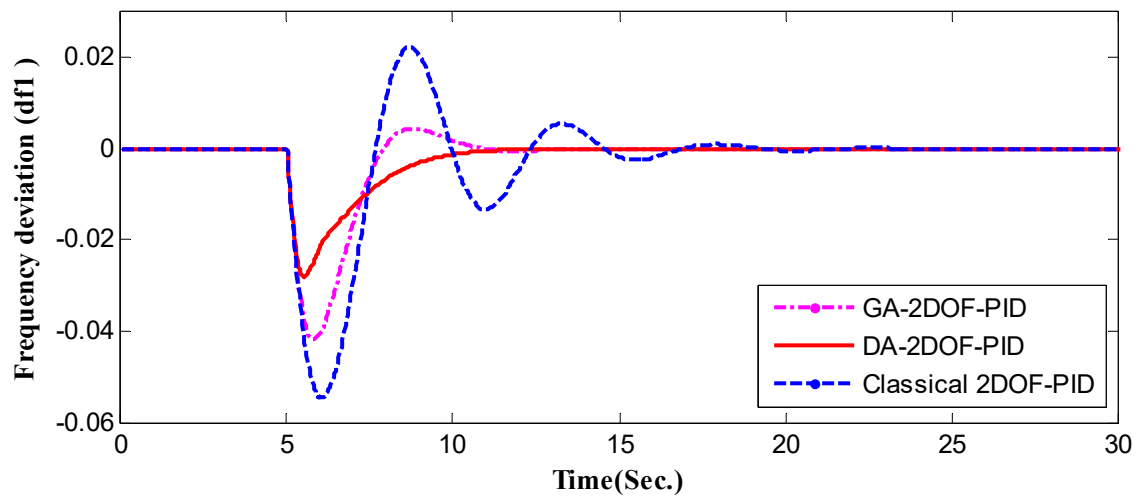


Figure 24. Δf_1 using GA-2DOF-PID, DA-2DOF-PID, and classical-2DOF-PID with IB-WGFF.

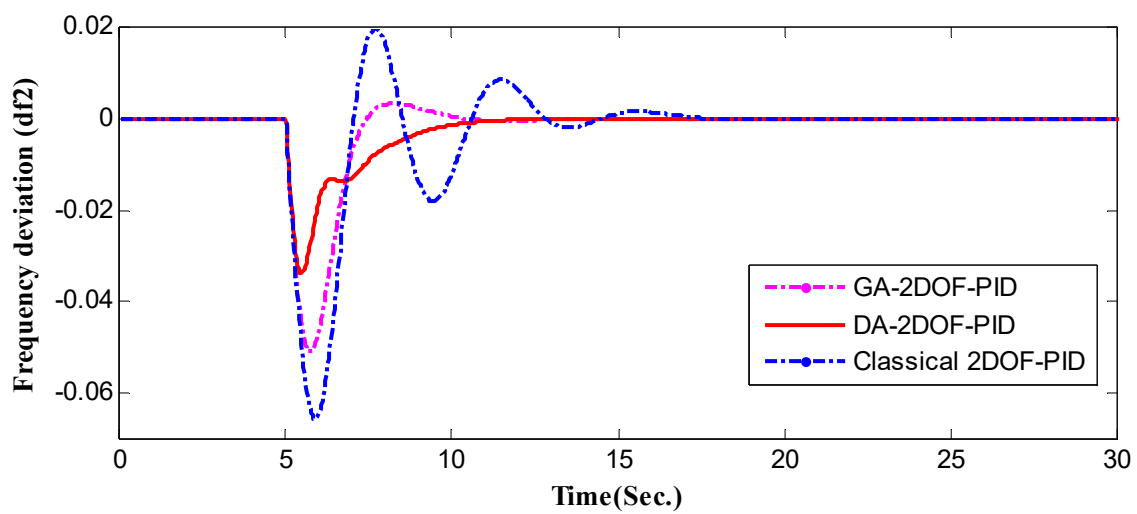


Figure 25. Δf_2 using GA-2DOF-PID, DA-2DOF-PID, and classical-2DOF-PID with IB-WGFF.

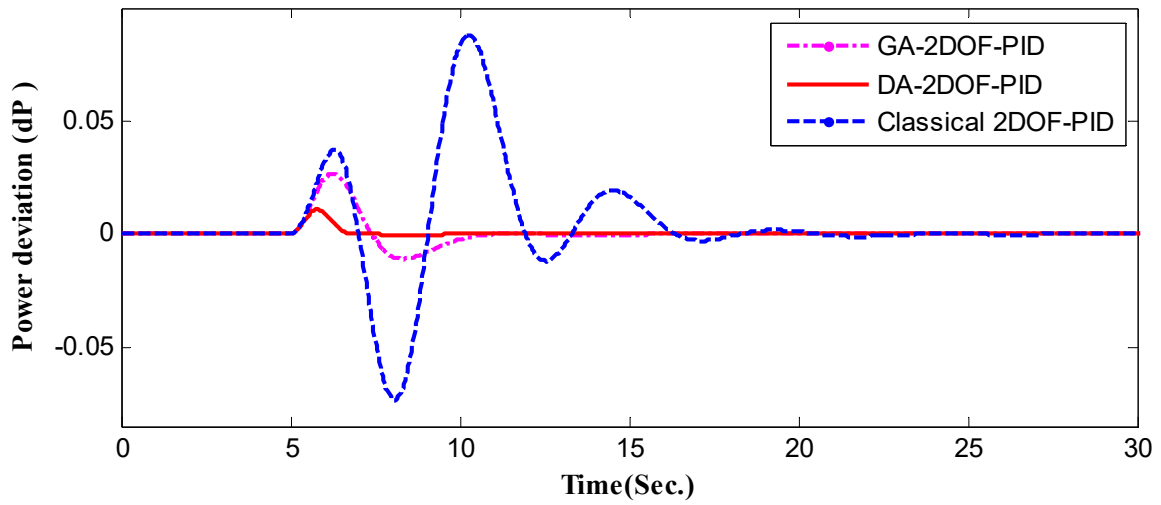


Figure 26. ΔP using GA-2DOF-PID, DA-2DOF-PID, and classical-2DOF-PID with IB-WGFF.

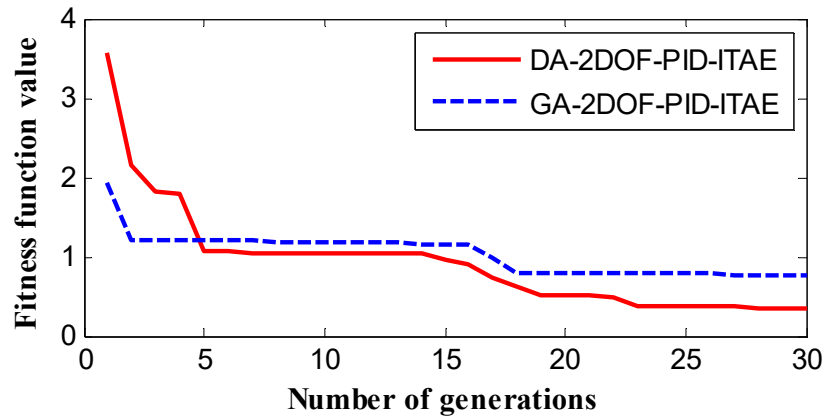


Figure 27. Comparative graph for the fitness function value using ITAE.

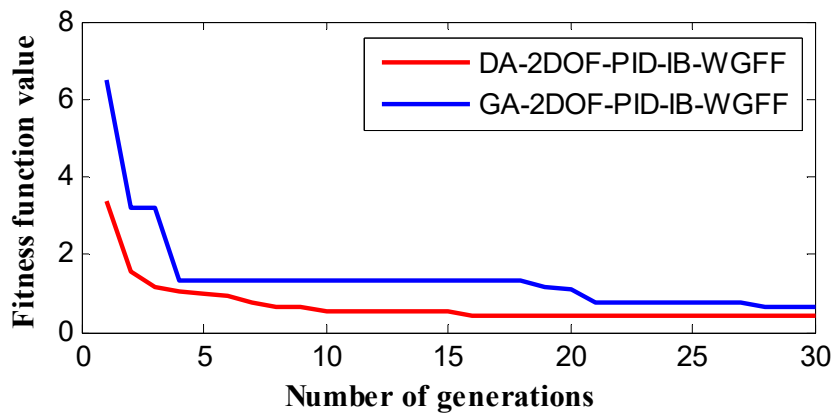


Figure 28. Comparative graph for the fitness function value using proposed IB-WGFF.

From Table 8 and Figures 18–20, it is found that the dynamic response of Δf_2 , Δf_1 , and ΔP , under GA-2DOF-PID-IB-WGFF controller is better than the conventional 2DOF-PID and GA-DOF-PID-IB-ITAE. It has smaller overshoot, undershoot, settling time, and fitness function value.

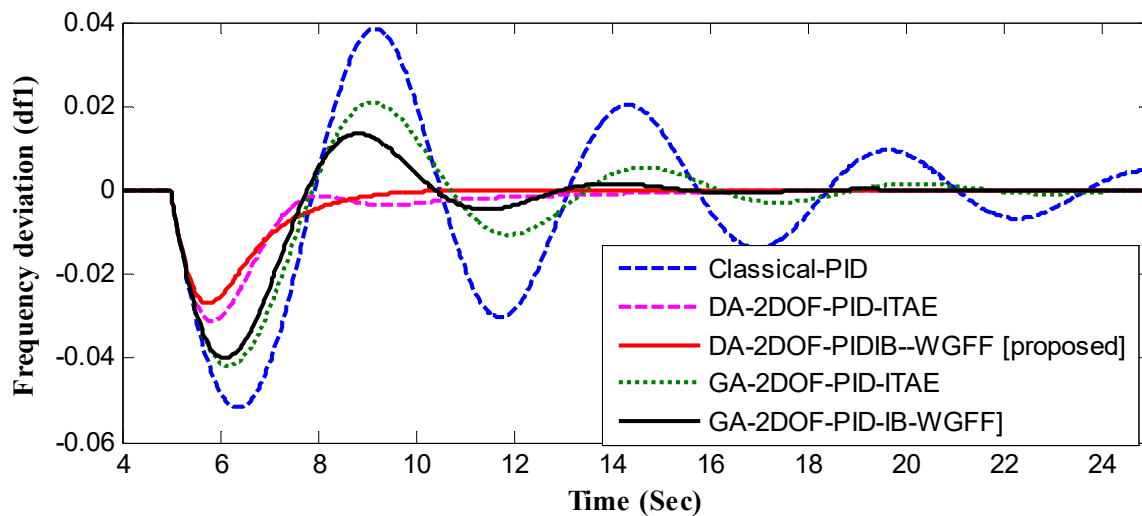


Figure 29. Frequency deviation (Δf_1) of area 1 under parameter perturbations.

It is found, from Figures 21–23, that the dynamic response of Δf_2 , Δf_2 and ΔP , using the DA-2DOF-PID-ITAE controller is better than the classical 2DOF-PID and GA-DOF-PID-IB-ITAE controllers.

Figures 24–26 and Table 8 indicated that the dynamic performance of the system, implementing the proposed DA-2DOF-PID-IB-WGFF, is better than the classical 2DOF-PID and the GA-2DOF-PID-IB-WGFF.

Finally, it is concluded that the dynamic performance of the system, implementing the proposed DA-2DOF-PID-IB-WGFF, is the best in terms of overshoot (zero), undershoot (0.0244), settling time (1.543), and fitness function value (0.399303).

Figure 27 indicates a graph between the fitness function value versus the generations number using GA and DA in case of the ITAE fitness function. Figure 28 shows a graph using GA and DA in case of the proposed IB-WGFF. It is found, from Figures 27 and 28, that the speed of convergence of DA is higher than GA in case of ITAE and the Proposed IB-WGFF. In addition, the DA has a value of fitness function of (0.399303) which is better than the value (0.657643) obtained in the case of GA.

6. Verification of the Proposed Control Scheme

This section of the article is dedicated for demonstrating the performance and verifying the superiority and robustness of the proposed control scheme under the parameters perturbations and load disturbances. Verification is done under the same parameters of controllers designed in Section 5.5 and indicated in Table 8. The following subsections demonstrates the dynamic response of the two-area power system (Δf_2 , Δf_2 , and ΔP) under parameters perturbations and load disturbances.

6.1. Parameters Perturbations

The parameters of the interconnected power system are constantly varying, this may seriously affect the system performance. Robustness against dynamic faults, uncertainties, and environmental changes is one of the essential gains of using the AI control approaches. To verify the stability, efficacy, and robustness of the proposed DA-2DOF-PID control scheme, the parameters (R , B , H , D , T_g , T_t , and T_{12}) of the studied system given in Figure 5, were significantly changed according to Table 9. The dynamic responses of Δf_2 , Δf_2 , and ΔP of the system, after implementing these changes under the application of the same conventional 2DOF-PID, DA-2DOF-PID-ITAE, GA-2DOF-PID-ITAE, GA-2DOF-PID-IB-WGFF, and the proposed DA-2-DOF-PID-IB-WGFF are demonstrated in Figures 29–31, respectively.

Table 9. Power system parameter variations.

Parameter	Variation Range (%)	Parameter	Variation Range (%)
$R_1 = 2.4;$	+40% (3.36)	$D_2 = 0.90;$	+10% (0.99)
$D_1 = 0.60;$	−40% (0.36)	$H_2 = 4.0;$	+10% (4.4)
$H_1 = 5.0;$	+50% (7.5)	$T_{g2} = 0.30;$	−10% (0.33)
$T_{g1} = 0.20;$	+10% (0.22)	$T_{i2} = 0.60;$	+10% (0.66)
$T_{i1} = 0.50;$	+25% (0.625)	$B_2 = 16.90;$	+20% (20.28)
$B_1 = 20.1;$	10% (22.11)	$T_{12} = 0.545;$	+10% (0.5995)
$R_2 = 0.0625;$	−10% (0.05625)		

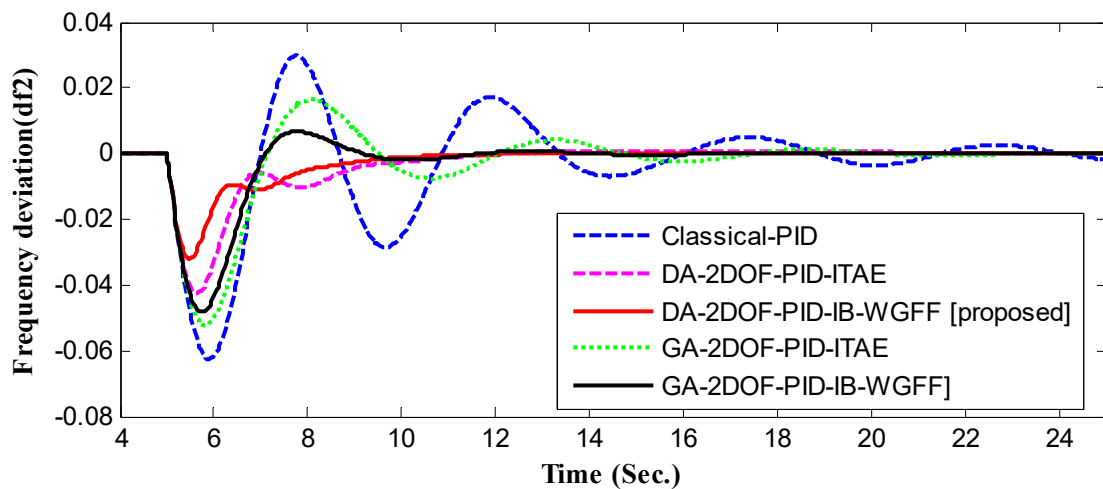


Figure 30. Frequency deviation (Δf_2) of area 2 under parameter perturbations.

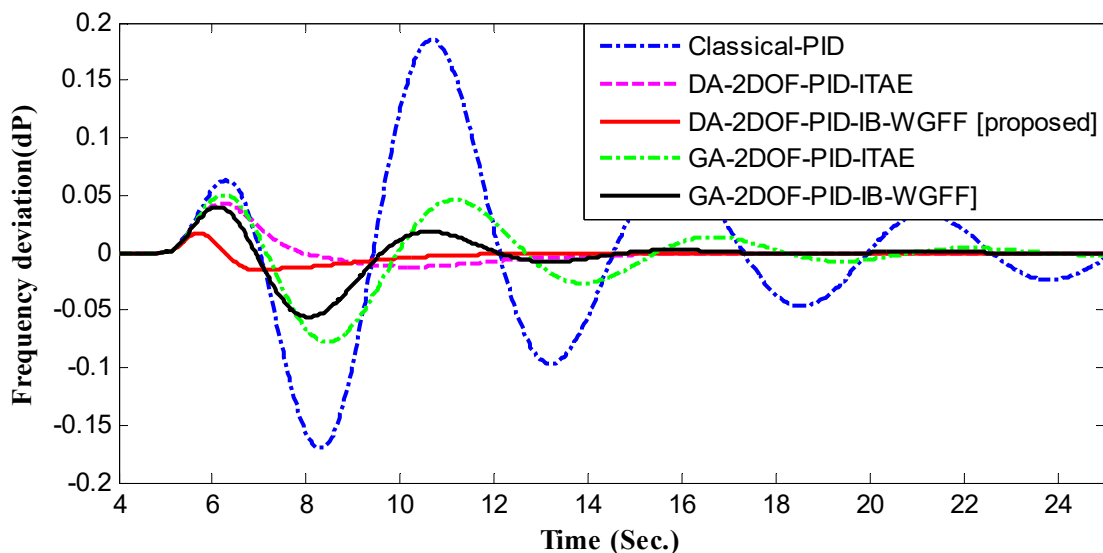


Figure 31. Tie-line power deviation (ΔP) after implementing parameter perturbations.

It can be concluded from Figures 29–31 that the conventional-2DOF-PID controller cannot handle the implemented system parameters perturbation given in Table 9. It is evident that the DA-2DOF-PID-ITAE, GA-2DOF-PID-ITAE, and GA-2DOF-PID-IB-WGFF controllers can follow and handle the implemented perturbations on the parameters but the dynamic response of the proposed 2DOF-PID control scheme tuned using the IB-WGFF (for

$C_1 = 0.5$ and $C_2 = 0.5$) is most robust and the smoothest one. It has the smallest undershoot, overshoot, and settling time.

6.2. The Impact of the Parameters Perturbations

This case tested the impact of the parameters perturbations on the studied two-area power system. This case was checked because it can generate high changes in the power system dynamic. In this case, the same load was applied allowing the uncertainties shown in Table 9. The frequency performance of the system against these changes was tested. Figure 32 shows the frequency response of the nominal and perturbed system under the proposed 2DOF-PID optimized using DA via the IB-WGFF. It is concluded, from Figure 32, that the proposed control scheme effectively enhances the dynamic performance. These results prove the significant role of the proposed scheme in supporting the power system frequency that occurs with highly disrupting conditions.

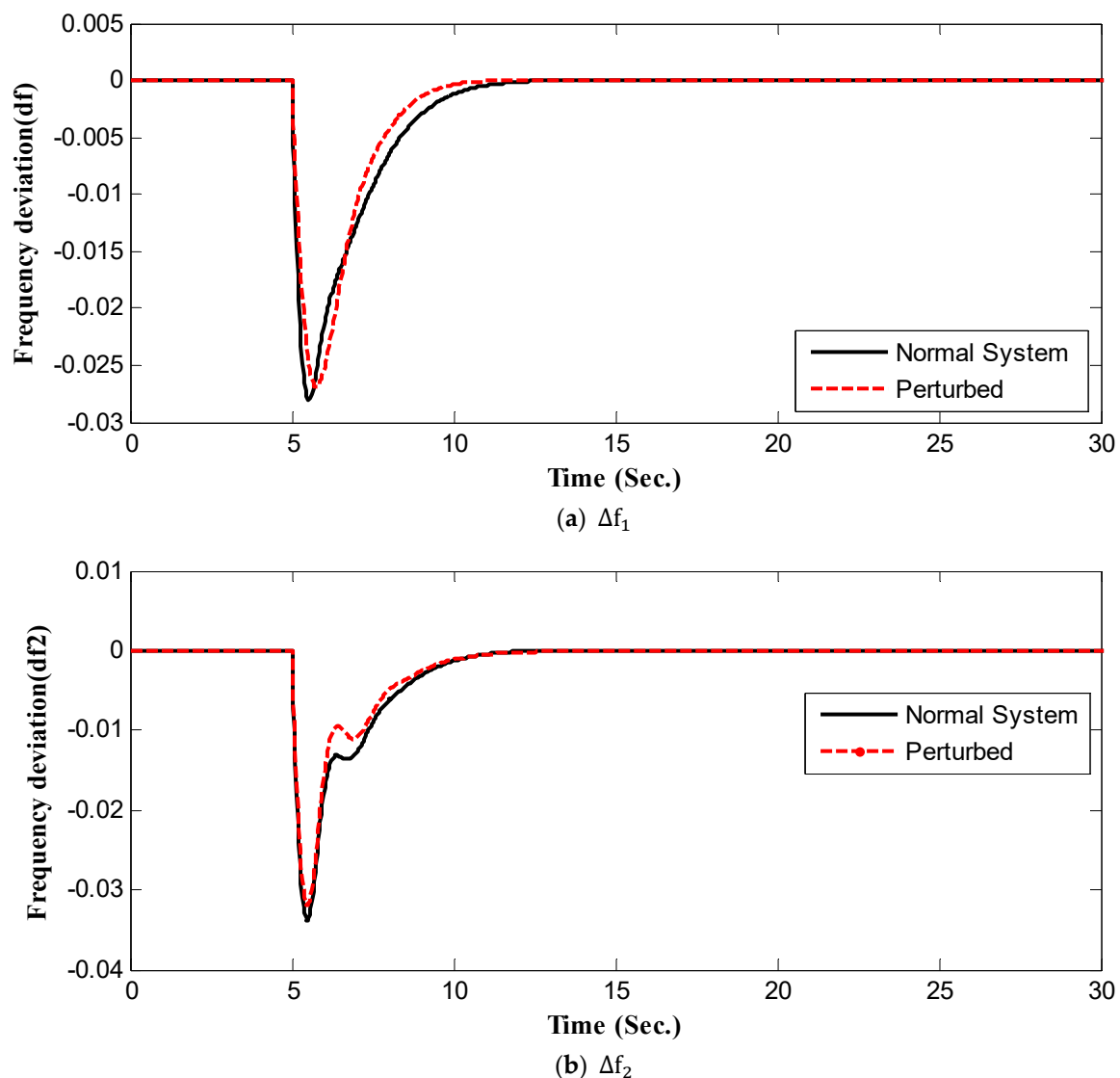
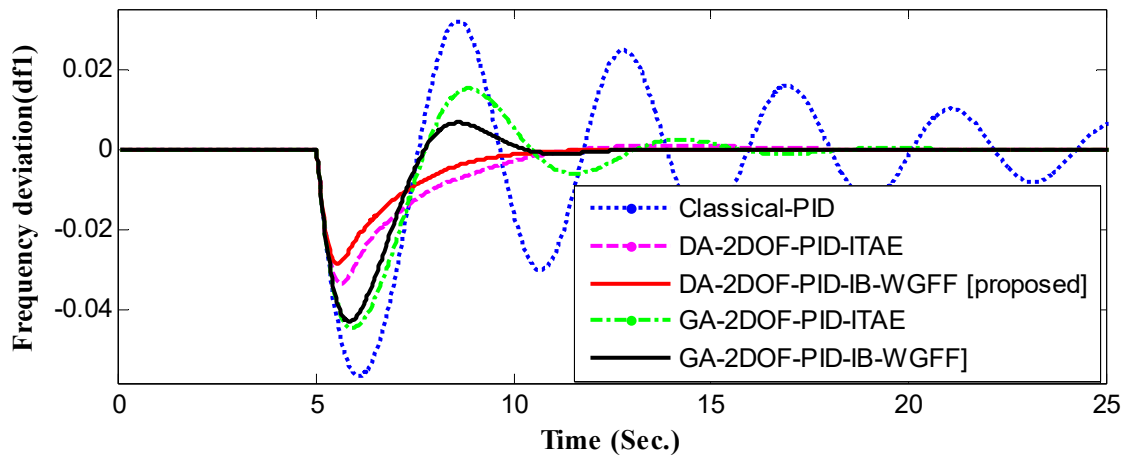


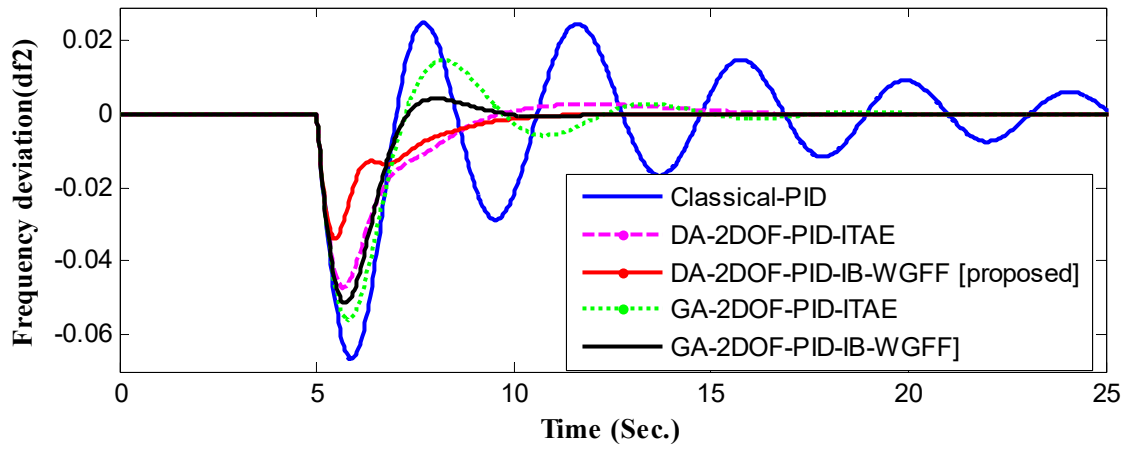
Figure 32. Dynamic response under normal and perturbed system using the proposed scheme.

6.3. Effect of Parameter Variation on System Response

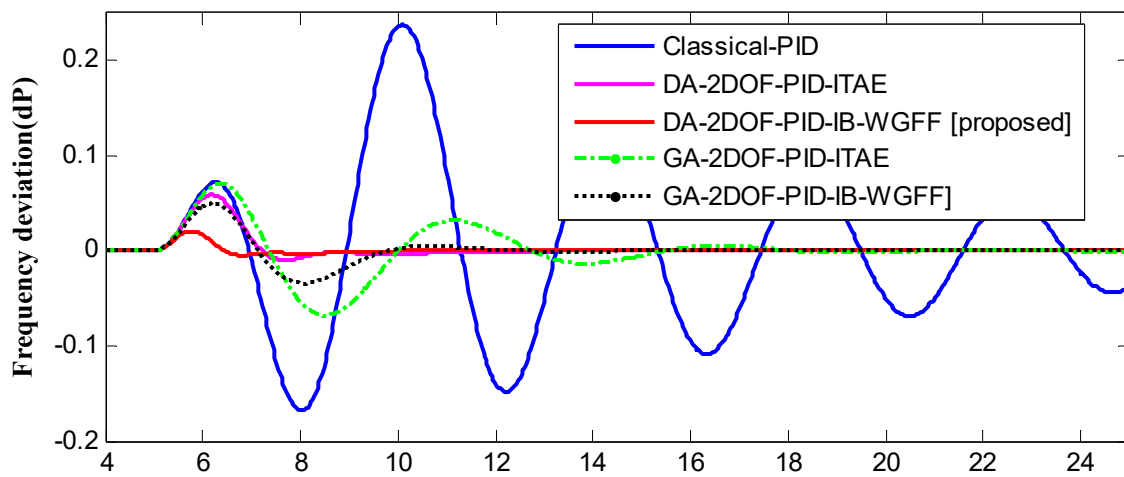
Figure 33 indicates the dynamic response of frequency for the first area with 50% increase in T_{12} . The dynamic response of the system under the proposed DA-2DOF-PID is more robust and provides better performance compared to the other controllers.



(a) Δf_1



(b) Δf_2



(c) ΔP

Figure 33. Dynamic Response due to the increase in T_{12} by a value of 50%.

6.4. Disturbance Load

Load variation results in frequency and power variation which may affect the power quality and system stability. These effects may reduce the damping performance of the controlled power system and could even lead to instability in the power system if these changes exceed the allowable limits. To verify the robustness of the proposed control

scheme, a varying load disturbance shown in Figure 34 under the same parameters obtained in Section 5.5 is implemented to the two-area power system shown in Figure 5.

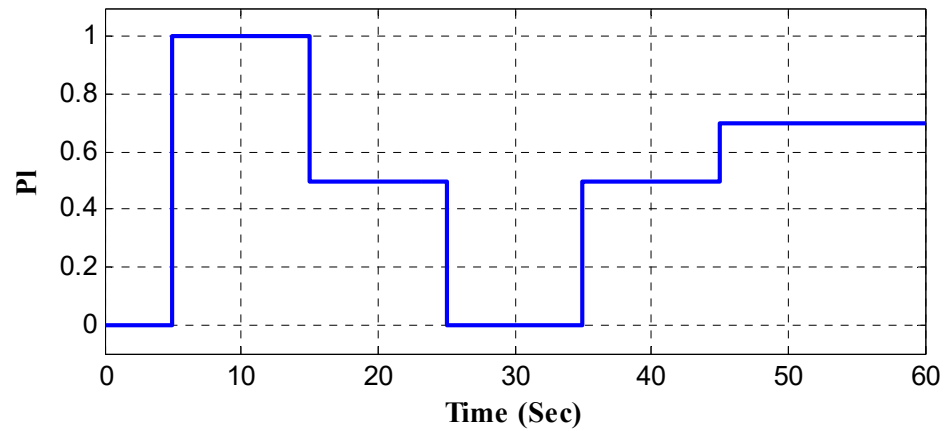


Figure 34. Implemented varying load disturbance (PL).

In this scenario, the ability of the proposed 2DOF-PID tuned using the designed IB-WGFF, under the effect of radical multi-step load disturbance, was evaluated and proved. The step load is applied to the studied system with varying step pattern increasing at the time instants $t = 5$ s, 35 s, and 45 s and decreasing at $t = 15$ and 25 s. Figures 35–37 indicate the dynamic of the two area power system implementing the conventional 2DOF-PID, the DA-2DOF-PID-ITAE, the GA-2DOF-PID-ITAE, GA-2DOF-PID-IB-WGFF, and the DA-2DOF-PID-IB-WGFF (for $C_1 = 0.5$ and $C_2 = 0.5$).

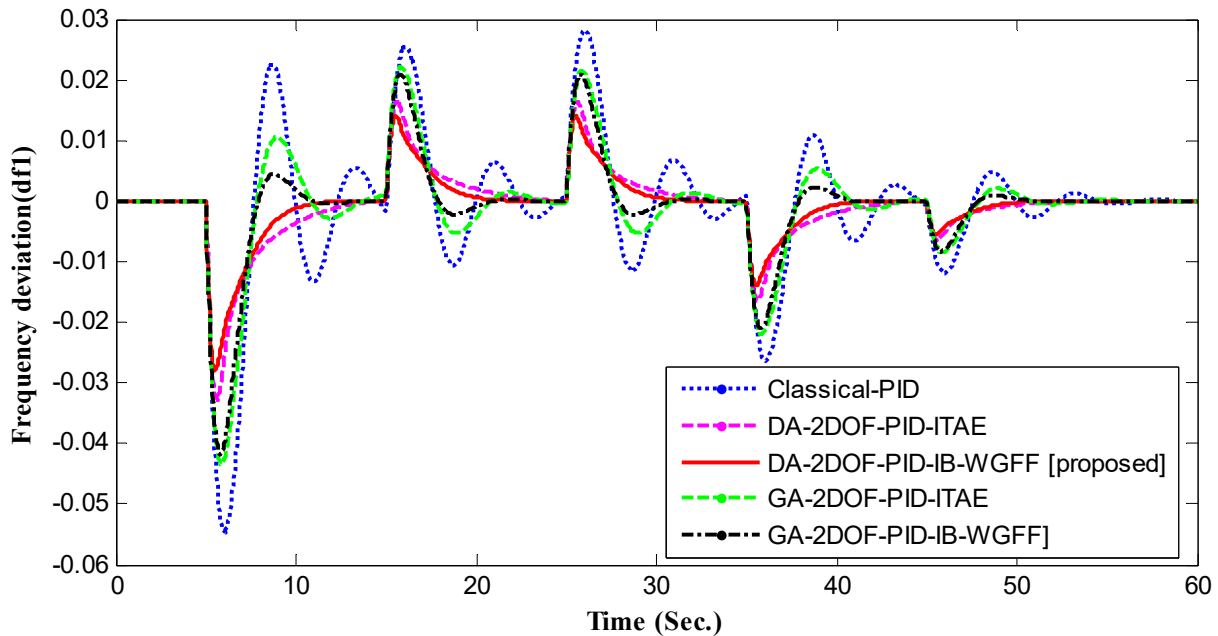


Figure 35. Δf_1 for area 1 under load disturbances.

It is evident that the dynamic behaviors of the power and frequency, under the proposed DA-2DOF-PID-IB-WGFF, have minimum deviations in comparison with the dynamics of all other implemented controllers. The proposed DA-2DOF-PID-IB-WGFF also have the fastest control action.

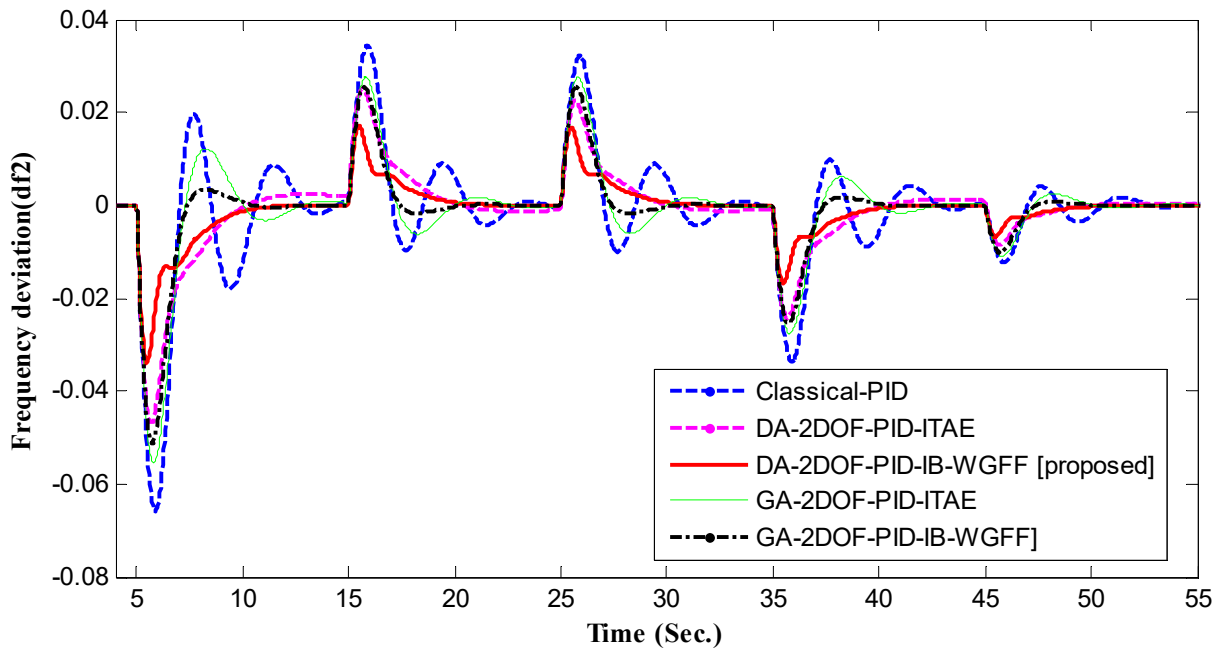


Figure 36. Δf_2 for Area 2 under load disturbances.

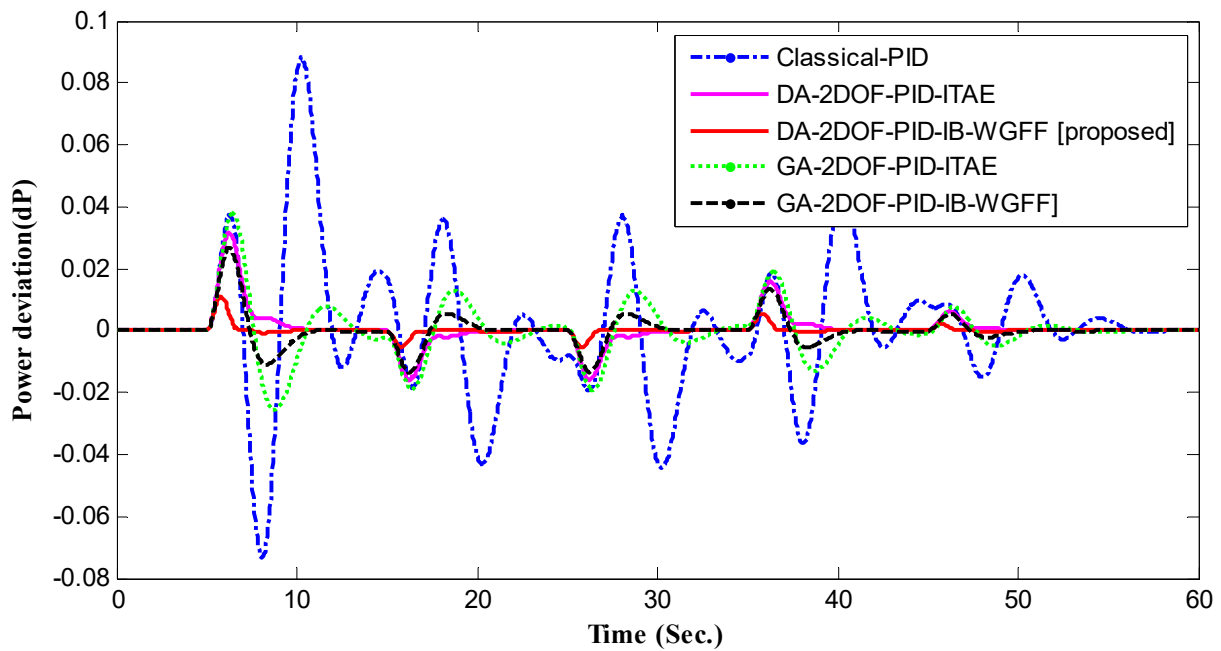


Figure 37. ΔP under load disturbances using different controllers.

It is obvious from Figures 35 and 36 that the novel proposed DA-2DOF-PID PID control scheme tuned via the IB-WGFF (for $C_1 = 0.5$ and $C_2 = 0.5$) can robustly keep the deviations in frequency within values between -0.028 and $+0.012$ for area1 and within values between -0.038 and 0.017 for area2 with the smoothest and fastest settling time. Contrariwise, under the DA-2-DOF-PID controller tuned via the ITAE comes in the second performance with deviations in frequency within values between -0.032 and 0.013 for area1 and within values between -0.044 and 0.024 for area2. The GA-2DOF-PID tuned via the IB-WGFF comes in the third order of performance with deviations in frequency within values between -0.041 and 0.021 for area1 and within values between -0.052 and 0.027 for area2. The GA-2DOF-PID tuned via the ITAE comes in the fourth order of performance

with deviations in frequency within values between -0.043 and 0.023 for area1 and within values between -0.058 and 0.031 for area2. The conventional-2DOF-PID comes in the fifth order of performance with deviations in frequency within values between -0.056 and 0.028 for area1 and within values between -0.068 and 0.038 for area2.

It is evident from Figure 37 that that the new proposed DA-2DOF-PID PID control scheme tuned via the IB-WGFF (for $C_1 = 0.5$ and $C_2 = 0.5$) can robustly keep the power deviation (ΔP) within values of about -0.005 and 0.008 pu. The other controllers can restore the tie-line power dynamics to its steady state of zero value but with high undershoots and overshoots and with longer settling times.

Again, it is concluded From Figures 35–37 that when a varying load is applied to the two-area power system, the DA-2DOF-PID controller tuned via the proposed IB-WGFF (for $C_1 = 0.5$ and $C_2 = 0.5$) is the best controller in terms of the overshoot, undershot, and settling time. Therefore, it evident, from the above discussion, that the dynamic performance of the system is improved implementing the proposed DA-2-DOF-PID controller tuned via the designed IB-WGFF.

7. Conclusions

In this article, an improved 2DOF-PID controller is designed for frequency/power control of a two-area interconnected power system. The implemented 2DOF-PID controller is optimized using Dragonfly Algorithm via the proposed IB-WGFF. For comparison, the result of the proposed controller is compared with the results of the classical-2DOF-PID controller and the 2DOF-PID tuned using Dragonfly Algorithm and Genetic Algorithm (GA) via the most common performance criterion used in the literature (i.e., ISE, ITAE, ITSE, and IAE). The simulation results proved that the proposed control scheme is better than the classical 2DOF-PID and the 2DOF-PID controllers tuned using DA and GA via the ITAE, ISE, IAE, and the ITSE. The proposed 2-DOF-PID controller is the smoothest and the best in overshoot, undershot, and settling time, and steady-state error. For proving the robustness and adaptive property of the proposed controller, the frequency deviation and the tie-line power of the two-area system are verified under the implementation of the same controllers for load disturbances and parameters perturbations. It is concluded that the 2DOF-PID control scheme tuned using the Dragonfly Algorithm via the proposed IB-WGFF (for $C_1 = 0.5$ and $C_2 = 0.5$) is the best controller in suppressing the frequency oscillations and tie-line power fluctuations under the load disturbance and system uncertainties.

Author Contributions: Conceptualization, A.M.A.-h., A.E.-S. and A.Y.A.; methodology, A.M.A.-h.; software, A.M.A.-h.; validation, A.M.A.-h., A.E.-S., A.Y.A.; formal analysis, A.M.A.-h.; investigation, A.M.A.-h.; resources, A.M.A.-h.; data curation, A.M.A.-h., A.E.-S. and A.Y.A.; writing—original draft preparation, A.M.A.-h.; writing—review and editing, A.Y.A., A.E.-S.; visualization, A.M.A.-h.; supervision, A.Y.A., A.E.-S.; project administration, A.Y.A., A.E.-S.; funding acquisition, A.Y.A. and A.E.-S. All authors have read and agreed to the published version of the manuscript.

Funding: This research received no external funding.

Data Availability Statement: Not applicable.

Conflicts of Interest: The authors declare no conflict of interest.

References

1. Essiet, I.O.; Sun, Y.; Wang, Z. Optimized energy consumption model for smart home using improved differential evolution algorithm. *Energy* **2019**, *172*, 354–3651. [[CrossRef](#)]
2. Tungadio, D.H.; Bansal, R.C.; Siti, M.W. Energy flow estimation-control of two interconnected microgrid. *J. Energy S. Afr.* **2008**, *29*, 69–80. [[CrossRef](#)]
3. Barakat, M. Novel chaos game optimization tuned-fractional-order PID fractional-order PI controller for load–frequency control of interconnected power systems. *Prot. Control Mod. Power Syst.* **2022**, *7*, 16. [[CrossRef](#)]
4. Kumar, N.; Malik, H.; Singh, A.; Alotaibi, M.A.; Nassar, M.E. Novel Neural Network-Based Load Frequency Control Scheme: A Case Study of Restructured Power System. *IEEE Access* **2021**, *9*, 162231–162242. [[CrossRef](#)]

5. Saxena, S. Load frequency control strategy via fractional order controller and reduced-order modeling. *Int. J. Electr. Power Energy Syst.* **2019**, *104*, 603–6014. [[CrossRef](#)]
6. Barakat, M.; Donkol, A.; Hamed, H.F.A.; Salama, G.M. Harris Hawks-Based optimization algorithm for automatic LFC of the interconnected power system using PD-PI cascade control. *J. Electr. Eng. Technol.* **2021**, *16*, 1845–1865. [[CrossRef](#)]
7. Lu, K.-D.; Zeng, G.-Q.; Zhou, W. Adaptive constrained population external optimisation-based robust proportional-integral-derivation frequency control method for an islanded microgrid. *IET Cyber Syst. Robot.* **2021**, *3*, 210–227. [[CrossRef](#)]
8. Hossain, S.A.; Roy, S.; Karmaker, A.; Islam, R. Performance improvement of PID controller for AVR system using Particle Swarm Optimization. In Proceedings of the 2015 International Conference on Advances in Electrical Engineering (ICAEE), Dhaka, Bangladesh, 17–19 December 2015.
9. Abdelaziz, A.Y.; Ali, E.S. Load Frequency Controller Design via Artificial Cuckoo Search. *Electr. Power Compon. Syst.* **2016**, *44*, 90–98. [[CrossRef](#)]
10. Fathy, A.; Kassem, A.M.; Abdelaziz, A.Y. Optimal Design of Fuzzy-PID Controller for Deregulated LFC of Multi-Area Power System via Mine Blast Algorithm. *Neural Comput. Appl.* **2020**, *32*, 4531–4551. [[CrossRef](#)]
11. Ebrahim, M.A.; Becherif, M.; Abdelaziz, A.Y. PID/FOPID-based Frequency control of zero-carbon multi-sources based interconnected power systems under deregulated scenarios. *Int. Trans. Electr. Energy Syst.* **2021**, *31*, e12712. [[CrossRef](#)]
12. Praveena, P.; Shubhanka, H.S.; Neha, V.; Prasath, P.; Veda, G.S. Load Frequency Control of Single Area System Using Ziegler-Nichols and Genetic Algorithm. *Asian J. Electr. Sci.* **2019**, *8*, 62–64. [[CrossRef](#)]
13. Kouba, N.E.Y.; Mena, M.; Hasni, M.; Boudour, M. Optimal control of frequency and voltage variations using PID controller based on Particle Swarm Optimization. In Proceedings of the 2015 4th International Conference on Systems and Control (ICSC), Sousse, Tunisia, 27–30 April 2015; pp. 424–429.
14. Arya, Y. AGC of two-area electric power systems using optimized fuzzy PID with filter plus double integral controller. *J. Frankl. Inst.* **2018**, *355*, 4583–4617. [[CrossRef](#)]
15. Gupta, D.; Goyal, G.; Kumar, J. An Optimized Fractional Order PID Controller for Integrated Power System. In *ICICCT 2019—System Reliability, Quality Control, Safety, Maintenance and Management, Proceedings of the ICICCT 2019 International Conference on Intelligent Computing and Communication Technologies, Hyderabad, India, 9–11 January 2019*; Gunjan, V.K., Diaz, V.G., Cardona, M., Solanki, V.K., Sunitha, K.V.N., Eds.; Springer: Singapore, 2019; pp. 663–672.
16. Lamba, R.; Singla, S.K.; Sondhi, S. Design of Fractional Order PID Controller for Load Frequency Control in Perturbed Two Area Interconnected System. *Electr. Power Compon. Syst.* **2019**, *47*, 998–1011. [[CrossRef](#)]
17. Singh, R.; Kesarwani, S.K.; Gupta, N.K.; Ashfaq, H. Design of 2-DOF PID Controller for Load Frequency Control of Two Area Power System using MFO Algorithm. *Int. J. Eng. Adv. Technol.* **2020**, *9*, 158–161. [[CrossRef](#)]
18. Karanam, A.N.; Shaw, B. A new two-degree of freedom combined PID controller for automatic generation control of a wind integrated interconnected power system. *Prot. Control Mod. Power Syst.* **2022**, *7*, 20. [[CrossRef](#)]
19. Kouba, N.E.Y.; Mena, M.; Hasni, M.; Boudour, M. A Novel Optimal Combined Fuzzy PID Controller Employing Dragonfly Algorithm for Solving Automatic Generation Control Problem. *Electr. Power Compon. Syst.* **2018**, *46*, 2054–2070. [[CrossRef](#)]
20. Guha, D.; Roy, P.K.; Banerjee, S. Quasi-oppositional JAYA optimized 2-degree-of-freedom PID controller for load-frequency control of interconnected power systems. *Int. J. Model. Simul.* **2022**, *42*, 63–85. [[CrossRef](#)]
21. Hassan, A.; Aly, M.; Elmelegi, A.; Nasrat, L.; Watanabe, M.; Mohamed, E.A. Optimal Frequency Control of Multi-Area Hybrid Power System Using New Cascaded TID-PI^λD^μN Controller Incorporating Electric Vehicles. *Fractal Fract.* **2022**, *6*, 548. [[CrossRef](#)]
22. Gheisarnejad, M. An effective hybrid harmony search and cuckoo optimization algorithm based fuzzy PID controller for load frequency control. *Appl. Soft Comput.* **2018**, *65*, 121–138. [[CrossRef](#)]
23. Barakat, M. Optimal design of fuzzy-PID controller for automatic generation control of multi-source interconnected power system. *Neural Comput. Appl.* **2022**, *34*, 18859–18880. [[CrossRef](#)]
24. Alhalabi, M.; Rashed, A.; Barham, Y.; Salim, R.; Ghazal, M. Two-Area Load Frequency Control for Power System Dynamic Performance Enhancement with a Graphical User Interface Integration. In Proceedings of the 2022 International Conference on Electrical, Computer and Energy Technologies (ICECET), Prague, Czech Republic, 20–22 July 2022.
25. Sahu, R.K.; Panda, S.; Padhanm, S. A novel hybrid gravitational search and pattern search algorithm for load frequency control of nonlinear power system. *Appl. Soft Comput.* **2015**, *29*, 310–327. [[CrossRef](#)]
26. Gbadega, P.A.; Saha, A.K. Load Frequency Control of a Two-Area Power System with a Stand-Alone Microgrid Based on Adaptive Model Predictive Control. *IEEE J. Emerg. Sel. Top. Power Electron.* **2021**, *9*, 7253–7263. [[CrossRef](#)]
27. Alaa Abdel-hamed, M.; Abou El-Eyoun, K.M.; Amged El-Wakeel, S. Optimized Control Scheme for Frequency/Power Regulation of Microgrid for Fault Tolerant operation. *Electr. Power Compon. Syst.* **2016**, *44*, 1429–1440. [[CrossRef](#)]
28. Tripathy, D.; Choudhury, N.D.; Sahu, B. Comparative performance assessment of several Fractional Order -Two Degree Freedom controllers tuned using GOA for LFC. *Procedia Comput. Sci.* **2020**, *167*, 2022–2032. [[CrossRef](#)]
29. Azzini, I.; Muresano, R.; Ratto, M. Dragonfly: A multi-platform parallel toolbox for MATLAB/Octave computer Languages. *Syst. Struct.* **2018**, *52*, 21–42.
30. Mirjalili, S. Dragonfly algorithm: A new meta-heuristic optimization technique for solving single-objective, discrete, and multiobjective problems. *Neural Comput. Appl.* **2015**, *27*, 1053–1073. [[CrossRef](#)]
31. Venkatesh, M.; Sudheer, G. Optimal Load Frequency Regulation of Micro-Grid Using Dragonfly Algorithm. *Int. Res. J. Eng. Technol.* **2017**, *4*, 978–981.

32. Gheisarnejad, M.; Khooban, M.H. Design an optimal fuzzy fractional proportional integral derivative controller with derivative filter for load frequency control in power systems. *Trans. Inst. Meas. Control* **2019**, *4*, 2563–2581. [[CrossRef](#)]
33. Fathy, A.; Yousri, D.; Rezk, H.; Thanikanti, S.B.; Hasanien, H.M. A Robust Fractional-Order PID Controller Based Load Frequency Control Using Modified Hunger Games Search Optimizer. *Energies* **2022**, *15*, 361. [[CrossRef](#)]
34. Rabindra, K.S.; Tulasichandra, S.G.; Sidhartha, P. Automatic generation control of multi-area power systems with diverse energy sources using Teaching Learning Based Optimization algorithm. *Eng. Sci. Technol. Int. J.* **2016**, *19*, 113–134.
35. Ali, T.; Malik, S.A.; Hameed, I.A.; Daraz, A.; Mujlid, H.; Azar, A.T. Load Frequency Control and Automatic Voltage Regulation in a Multi-Area Interconnected Power System Using Nature-Inspired Computation-Based Control Methodology. *Sustainability* **2022**, *14*, 12162. [[CrossRef](#)]
36. Elwakel, A.S.; Ellissy, A.; Abdelhamed, A.M. A Hybrid Bacterial Foraging-Particle Swarm Optimization Technique for Optimal Tuning of Proportional-Integral-Derivative Controller of a Permanent Magnet Brushless DC Motor. *Electr. Power Compon. Syst.* **2015**, *3*, 309–319. [[CrossRef](#)]
37. Cam, E.; Gorel, G.; Mamur, H. Use of the Genetic Algorithm-Based Fuzzy Logic Controller for Load-Frequency Control in a Two Area Interconnected Power System. *Appl. Sci.* **2017**, *7*, 308. [[CrossRef](#)]

Disclaimer/Publisher’s Note: The statements, opinions and data contained in all publications are solely those of the individual author(s) and contributor(s) and not of MDPI and/or the editor(s). MDPI and/or the editor(s) disclaim responsibility for any injury to people or property resulting from any ideas, methods, instructions or products referred to in the content.